Saeed M, <u>Suzuki R</u>, Watanabe N, Masaki T, Tomonaga M, Muhammad A, Kato T, Matsuura Y, Watanabe H, Wakita T, Suzuki T. （鈴木）	Role of the ERAD pathway in degradation of hepatitis C virus envelope proteins and production of virus particles.	*J. Biol. Chem.*	286	37264-37 273	2011

IV. 研究成果の刊行物・別刷

Incorporation of Biaryl Units into the 5′ and 3′ Ends of Sense and Antisense Strands of siRNA Duplexes Improves Strand Selectivity and Nuclease Resistance

Kayo Yoshikawa,[†] Aya Ogata,[†] Chiho Matsuda,[§] Michinori Kohara,[§] Hideo Iba,[‖] Yukio Kitade,[†,‡] and Yoshihito Ueno*,[†,‡]

Department of Biomolecular Science, Faculty of Engineering, and United Graduate School of Drug Discovery and Medical Information Sciences, Gifu University, 1-1 Yanagido, Gifu 501-1193, Japan, Department of Microbiology and Cell Biology, The Tokyo Metropolitan Institute of Medical Science, 2-1-6, Kamikitazawa, Setagaya-ku, Tokyo 156-0057, Japan, and Division of Host-Parasite Interaction, Department of Microbiology and Immunology, Institute of Medical Science, The University of Tokyo, 4-6-1 Shirokanedai, Minato-ku, Tokyo 108-8639, Japan.

Small interfering RNA (siRNA) is a noncoding RNA with considerable potential as a new therapeutic drug for intractable diseases. siRNAs can be rationally designed and synthesized if the sequences of the disease-causing genes are known. In this paper, we describe the synthesis and properties of siRNAs modified with biaryl units. We found that incorporation of biaryl units into the 5′ and 3′ ends of sense and antisense strands of siRNA duplexes improved strand selectivity and nuclease resistance.

INTRODUCTION

RNA interference (RNAi) is a biological process whereby double-stranded RNAs (dsRNAs) silence gene expression in a sequence-specific manner (*1*). Small RNAs, including small interfering RNA (siRNA) and microRNA (miRNA), are key intermediates in RNAi. They regulate gene expression through the RNA-induced silencing complex (RISC), which contains Argonaute proteins as core components. siRNAs hold considerable potential as new therapeutic drugs for intractable diseases, because they can be rationally designed and synthesized if the sequences of disease-causing genes are known (*2–6*).

One strand from an siRNA or miRNA duplex is selected and loaded onto RISC to become mature siRNA or miRNA. It has been suggested that RISC preferentially selects and incorporates one of two strands of the siRNA duplex, depending on its thermodynamic features. The strand with thermodynamically lower stability in its 5′-terminus (the guide strand) preferentially binds the RISC and becomes functional, whereas the other strand (the passenger strand) is degraded (*7–9*). However, it has recently become clear that strand selection does not always follow this rule (*1–14*). Recently reported siRNA studies demonstrated that modifying the 5′-terminus of one strand with 5′-*O*-methyl efficiently specifies its antisense strand to be loaded onto RISC despite thermodynamic disadvantages (*15*), because 5′-*O*-methyl inhibits phosphorylation of the 5′-terminus, which is an important factor for RISC loading (*16–20*).

We have reported the synthesis of DNAs containing biaryl units, **3** and **5**, which comprised benzene and naphthalene or pyrene residues (Figure 1). The biaryl units thermally and thermodynamically stabilized DNA/DNA duplexes (*21*). We
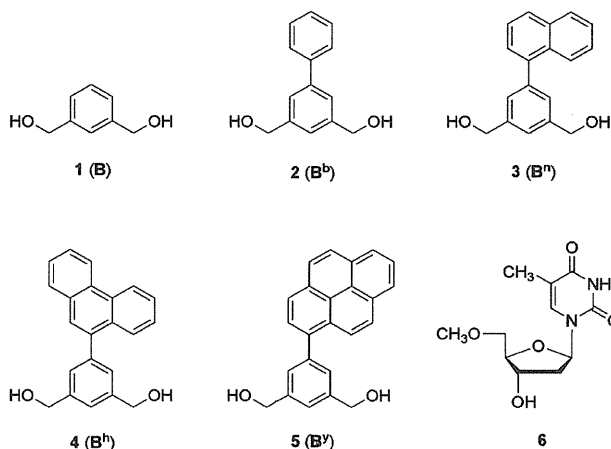

Figure 1. Structures of the aromatic compounds and modified nucleoside used in this study.

have also succeeded in improving siRNA nuclease resistance by introduction of bis(hydroxymethyl)benzene (**1**) instead of thymidine at 3′-overhangs without reducing RNAi-inducing activity (*22*). From these results and background information, we planned the synthesis of siRNAs with biaryl units at the 5′ and 3′ ends of sense and antisense strands of siRNA duplexes, respectively. We expected that thermal and thermodynamic stabilities of the 5′ regions of siRNA sense strands would be increased by these biaryl modifications. Phosphorylation of the 5′ ends of sense strands, an important factor for RISC loading, was expected to be inhibited by biaryl protection of 5′-hydroxyls. We anticipated that these modifications would enhance RISC loading of antisense strands of siRNA duplexes, suppressing off-target effects induced by sense strands. We also anticipated improved nuclease resistance in biaryl-modified siRNAs, which is important for the therapeutic application of synthetic siRNAs.

In this paper, we report the synthesis and properties of siRNA duplexes which carry biaryl units at the 5′ and 3′ ends of sense and antisense strands, respectively. We assessed the gene

* To whom correspondence should be addressed. Phone: +81-58-293-2639. Fax: +81-58-293-2794. E-mail: uenoy@gifu-u.ac.jp.
 † Department of Biomolecular Science, Faculty of Engineering, Gifu University.
 ‡ United Graduate School of Drug Discovery and Medical Information Sciences, Gifu University.
 § The Tokyo Metropolitan Institute of Medical Science.
 ‖ The University of Tokyo.

Scheme 1[a]
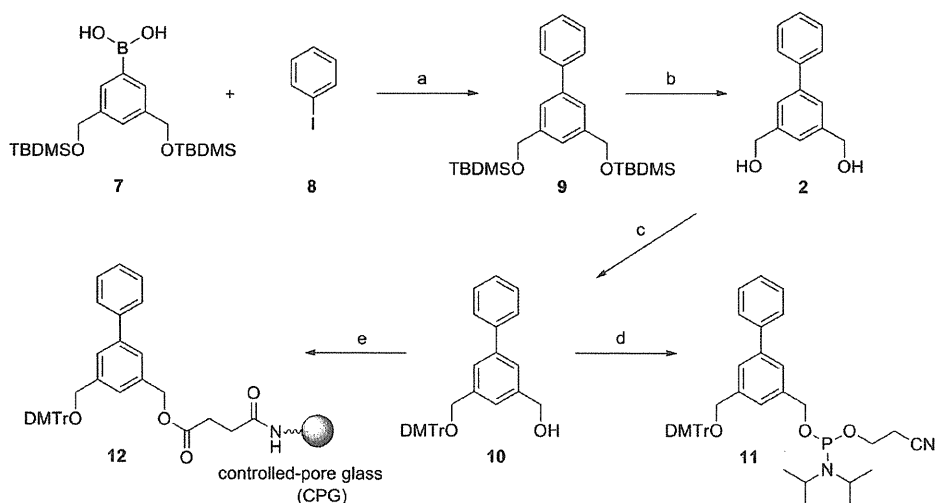
[a] Reagents and conditions: (a) PdCl₂(dppf)·CH₂Cl₂, NaOH, THF/H₂O (5:1 v/v), 65 °C, 24 h; (b) TBAF, THF, rt, 2 h, 93% from **7**; (c) DMTrCl, pyridine, rt, 4 h, 52%; (d) chloro(2-cyanoethoxy)(*N,N*-diisopropylamino)phosphane, *i*-Pr₂NEt, THF, rt, 1 h, 88%; (e) (1) succinic anhydride, DMAP, pyridine, rt, 24 h; (2) CPG, EDCI, DMF, rt, 48 h, 49 μmol/g loading amount.

Scheme 2[a]
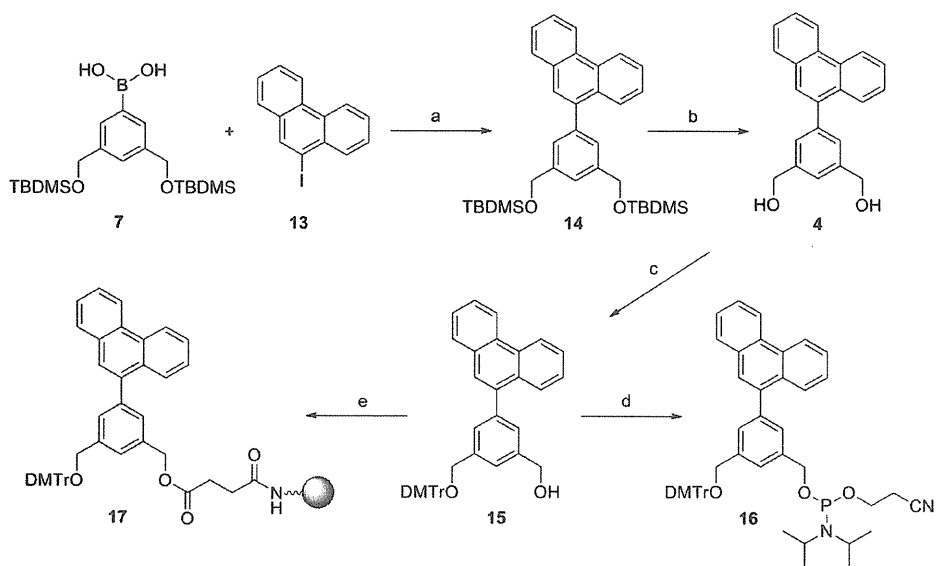
[a] Reagents and conditions: (a) PdCl₂(dppf)·CH₂Cl₂, NaOH, THF/H₂O (5:1 v/v), 65 °C, 24 h; (b) TBAF, THF, rt, 2 h, 60% from **7**; (c) DMTrCl, pyridine, rt, 3 h, 61%; (d) chloro(2-cyanoethoxy)(*N,N*-diisopropylamino)phosphane, *i*-Pr₂NEt, THF, rt, 1 h, 74%; (e) (1) succinic anhydride, DMAP, pyridine, rt, 24 h; (2) CPG, EDCI, DMF, rt, 48 h, 45 μmol/g loading amount.

silencing activities of the modified siRNAs by a dual-luciferase assay. We also assessed the nuclease-resistance of the modified siRNAs.

RESULTS AND DISCUSSION

Design and Synthesis of siRNAs. The Argonaute proteins are core components of RISC, which is responsible for mRNA cleavage in the RNAi pathway. The proteins are composed of PAZ, Mid, and PIWI domains. X-ray structural analysis and a nuclear magnetic resonance (NMR) study have revealed that the 3′-overhang region of a guide strand of siRNA is recognized by the PAZ domain and the 2-nucleotide (nt) 3′-overhang is accommodated by a binding pocket composed of hydrophobic amino acids (*23−26*). In order to estimate the appropriate size for biaryl units in the 3′-overhang region, we assessed the silencing activities of siRNAs which carried various types of biaryl units at the 3′-overhangs.

We assessed the biaryl units **2** (B^b), **3** (B^n), **4** (B^h), and **5** (B^y), comprising benzene and benzene, naphthalene, phenanthrene, or pyrene residues, to determine the appropriate size for the 3′-overhang regions. Phosphoramidites of **3** and **5** were synthesized according to a previously reported method (*21*). Phosphoramidites of **2** and **4** and solid supports carrying **2** or **4** were synthesized according to the methods shown in Schemes 1 and 2. An arylboronic acid derivative **7** was coupled with iodobenzene (**8**) in the presence of PdCl₂(dppf) (dppf stands for 1,1′-bis(diphenylphosphanyl)ferrocene) at 65 °C; this coupling reaction produced the biaryl derivative **9**; subsequently, **9** was desilylated by treatment with tetra-*n*-butylammonium fluoride (TBAF) to give a 93% yield of biaryl unit **2**. One out of the two hydroxy groups of **2** was protected by a 4,4′-dimethoxytrityl (DMTr) group to give a 52% yield of mono-DMTr derivative **10**. **10** was phosphitylated by the standard procedure to produce the corresponding phosphoramidite **11** at

Table 1. Sequences of ONs and siRNAs[a]

no. of siRNA	no. of ON	sequence
siRNA18	ON43	5'-GGCCUUUCACUACUCCUAC*tt*-3'
	ON44	3'-*tt*CCGGAAAGUGAUGAGGAUG-5'
siRNA19	ON45	5'-GGCCUUUCACUACUCCUACB^bB^b-3'
	ON46	3'-B^bB^bCCGGAAAGUGAUGAGGAUG-5'
siRNA20	ON47	5'-GGCCUUUCACUACUCCUACB^nB^n-3'
	ON48	3'-B^nB^nCCGGAAAGUGAUGAGGAUG-5'
siRNA21	ON49	5'-GGCCUUUCACUACUCCUACB^hB^h-3'
	ON50	3'-B^hB^hCCGGAAAGUGAUGAGGAUG-5'
siRNA22	ON51	5'-GGCCUUUCACUACUCCUACB^yB^y-3'
	ON52	3'-B^yB^yCCGGAAAGUGAUGAGGAUG-5'
siRNA23	ON53	F-5'-GGCCUUUCACUACUCCUAC*tt*-3'
	ON44	3'-*tt*CCGGAAAGUGAUGAGGAUG-5'
siRNA24	ON54	F-5'-GGCCUUUCACUACUCCUACB^bB^b-3'
	ON46	3'-B^bB^bCCGGAAAGUGAUGAGGAUG-5'
siRNA25	ON55	5'-CUUCUUCGUCGAGACCAUG*tt*-3'
	ON56	3'-*tt*GAAGAAGCAGCUCUGGUAC-5'
siRNA26	ON57	5'-B^bCUUCUUCGUCGAGACCAUG*tt*-3'
	ON56	3'-*tt*GAAGAAGCAGCUCUGGUAC-5'
siRNA27	ON58	5'-B^nCUUCUUCGUCGAGACCAUG*tt*-3'
	ON56	3'-*tt*GAAGAAGCAGCUCUGGUAC-5'
siRNA28	ON55	5'-CUUCUUCGUCGAGACCAUG*tt*-3'
	ON59	3'-*tt*GAAGAAGCAGCUCUGGUACB^b-5'
siRNA29	ON55	5'-CUUCUUCGUCGAGACCAUG*tt*-3'
	ON60	3'-*tt*GAAGAAGCAGCUCUGGUACB^n-5'
siRNA30	ON61	5'-UUUCACUACUCCUAC*tt*-3'
	ON62	3'-*tt*AAAGUGAUGAGGAUGCUCG-5'
siRNA31	ON63	5'-B^nUUUCACUACUCCUACGAGCBB-3'
	ON64	3'-BB^nAAAGUGAUGAGGAUGCUCG-5'
siRNA32	ON63	5'-B^nUUUCACUACUCCUACGAGCBB-3'
	ON65	3'-B^nB^nAAAGUGAUGAGGAUGCUCG-5'
siRNA33	ON66	5'-T^mUUCACUACUCCUACGAGC*tt*-3'
	ON62	3'-*tt*AAAGUGAUGAGGAUGCUCG-5'
siRNA34	ON67	5'-UAAGAUGUUCAUCGAGUCC*tt*-3'
	ON68	3'-*tt*AUUCUACAAGUAGCUCAGG-5'
siRNA35	ON69	5'-B^nUAAGAUGUUCAUCGAGUCCBB-3'
	ON70	3'-BB^nAUUCUACAAGUAGCUCAGG-5'
siRNA36	ON69	5'-B^nUAAGAUGUUCAUCGAGUCCBB-3'
	ON71	3'-B^nB^nAUUCUACAAGUAGCUCAGG-5'
siRNA37	ON72	5'-GUCUCGUAGACCGUGCAUCA*tt*-3'
	ON73	3'-*tt*CAGAGCAUCUGGCACGUAGU-5'
siRNA38	ON74	5'-GUCUCGUAGACCGUGCAUCABB-3'
	ON75	3'-BBCAGAGCAUCUGGCACGUAGU-5'
siRNA39	ON76	5'-B^nGUCUCGUAGACCGUGCAUCABB-3'
	ON77	3'-BB^nCAGAGCAUCUGGCACGUAGU-5'
siRNA40	ON76	5'-B^nGUCUCGUAGACCGUGCAUCABB-3'
	ON75	3'-BBCAGAGCAUCUGGCACGUAGU-5'
siRNA41	ON74	5'-GUCUCGUAGACCGUGCAUCABB-3'
	ON77	3'-BB^nCAGAGCAUCUGGCACGUAGU-5'
siRNA42	ON78	5'-B^nGUCUC<u>A</u>UAGG<u>CC</u>AUGC<u>G</u>UCABB-3'
	ON79	3'-BB^nCAGAG<u>U</u>AUC<u>C</u>GG<u>U</u>ACGC<u>A</u>GU-5'

[a] The small italic letters represent 2'-deoxyribonucleosides. The underlined letters indicate mismatched bases. F shows fluorescein.

Table 2. T_m Values[a]

no. of siRNA	T_m (°C)	ΔT_m (°C)
siRNA18	79.1	-
siRNA19	79.9	+0.8
siRNA20	80.7	+1.6
siRNA21	82.2	+3.1
siRNA22	82.8	+3.7

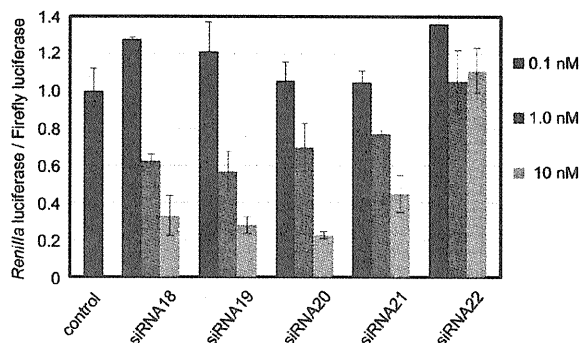[a] The experimental conditions are as described in the Experimental Section.

Figure 2. Dual-luciferase assay (1). The experimental conditions are as described in the Experimental Section.

an 88% yield. In a similar manner, phosphoramidite **16** was synthesized from 9-iodophenanthrene (**13**); the total yield of **16** was 27%.

To enable attachment to the solid support, the mono-DMTr derivative **10** was succinated to yield the corresponding succinate, which was linked to controlled pore glass (CPG) to create the solid support **12** linked to **10** (49 μmol/g). Similarly, the mono-DMTr derivative **15** was succinated and linked to the CPGs to yield the solid supports **17** linked to **15** (45 μmol/g). siRNA sequences used in this study are depicted in Table 1.

Thermal Denaturation Study of siRNAs. Thermal stability of biaryl-modified siRNAs was studied by thermal denaturation in 0.01 M sodium phosphate buffer (pH 7.0) containing 0.1 M NaCl (Table 2). The melting temperature (T_ms) of unmodified siRNA18 was 79.1 °C, while those of siRNAs **19**, **20**, **21**, and **22** were 77.9, 80.7, 82.2, and 82.8 °C, respectively. The siRNA duplexes were found to become more thermostable with increasing biaryl unit size. This result suggests that thermal stabilization of the duplexes is attributable to stacking interactions of the biaryl units with adjacent nucleotides.

Dual-Luciferase Assay. We assessed the silencing activity of modified siRNAs by performing a dual-luciferase assay using the psiCHECK-2 vector. siRNA sequences were designed to target *Renilla* luciferase. Reporter vectors and synthesized siRNA duplexes were cotransfected into HeLa cells, and luciferase activities were measured after 24 h. The signals of *Renilla* luciferase were normalized to those of firefly luciferase.

As shown in Figure 2, siRNA18, **19**, and **20**, which carried natural thymidines, B^bs or B^ns at their 3'-overhangs, effectively reduced luciferase activity in a dose-dependent manner. In contrast, the silencing activity of siRNA21, which contained B^h comprising a tricyclic phenanthrene residue, was apparently weaker than that of unmodified siRNA18. Further, siRNA22, which carried B^y with a tetracyclic pyrene residue, had no silencing activity. Thus, biaryl units smaller than the naphthalene type are acceptable for the 3'-overhang region of siRNAs. These results are consistent with a recent report from Somoza et al (*27*).

Microarray profiling studies have demonstrated that siRNAs may silence multiple genes in addition to the intended target (*28, 29*). This unintended (off-target) transcript silencing is a critical problem associated with RNAi-based therapeutic applications. Both the sense and antisense strands of an siRNA can contribute to the off-target effects. Thus, to minimize the extent of sense-strand incorporation into an activated RISC, we next examined the silencing activity of siRNAs, which involved the biaryl units at the 5' ends of sense or antisense strands of siRNA duplexes. We expected that inhibition of 5'-*O*-phosphorylation of sense strands with biaryl protection of 5'-hydroxyls would enhance RISC loading of antisense strands.

Figure 3a shows the results of siRNAs modified at the 5' ends of sense strands with biaryl units B^b and B^n, whereas Figure 3b represents those modified at the 5' ends of antisense strands. Modifications at the 5' ends of sense strands did not influence siRNA silencing activity, whereas modifications at the 5' ends of antisense strands markedly reduced silencing activity. Thus, it was found that the biaryl modifications at the 5'-termini of the sense strands could induce the antisense strand specificity of the siRNA duplexes.
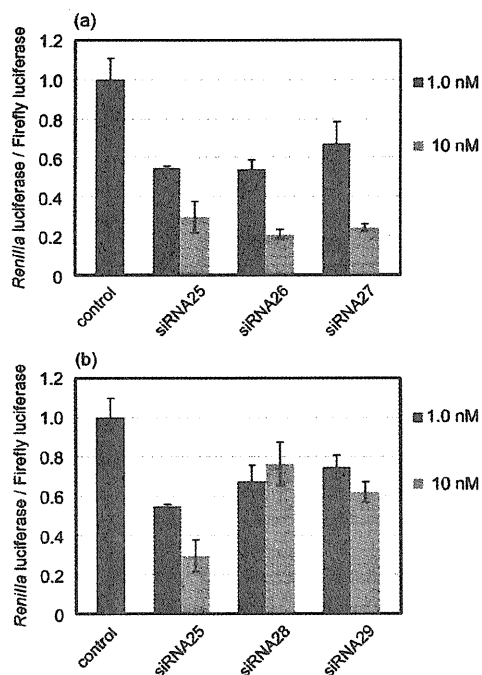
Figure 3. Dual-luciferase assay (2). (a) siRNAs modified at 5′-ends of passenger (sense) strands. (b) siRNAs modified at 5′-ends of guide (antisense) strands.

Next, we designed siRNAs which carried biaryl units at the 5′ and 3′ ends of sense and antisense strands, respectively. We speculated that incorporation of the biaryl units into the 5′ and 3′ ends of sense and antisense strands of siRNAs would increase the thermal and thermodynamic stabilities of the sense-strand 5′ siRNA regions. Further, introduction of the biaryl units at the 5′ ends of sense strands would inhibit phosphorylation, which is an important factor for RISC loading. We hypothesized that these modifications would work synergistically, creating more potent siRNAs.

We selected target sequences containing high frequencies of U and A bases, which are thought to be unsuitable targets for siRNA (Table 1). The results of dual-luciferase assays are shown in Figure 4a and b. Unmodified siRNA30 exhibited almost no silencing activity, whereas siRNA31 and 32 modified with **B** and **B^n** reduced luciferase activity in a dose-dependent manner (Figure 4a). Silencing activities of biaryl-modified siRNA31 and 32 were greater than that of siRNA33 containing 5′-*O*-methylthymidine at the 5′ end of the sense strand at all concentrations. This indicates that not only inhibition of phosphorylation, but also thermal stabilization of the 5′ regions of sense strands, contributes to improving siRNA silencing activity. Similarly, unmodified siRNA34 had almost no silencing activity, whereas biaryl-modified siRNA35 and 36 efficiently suppressed luciferase expression in a dose-dependent manner (Figure 4b). These results suggest that biaryl modification may provide a good method for improving siRNA silencing activities of sequences which are thought to be unsuitable siRNA targets.

Nuclease Resistance. Improving the nuclease resistance of siRNA is important for the therapeutic application of synthetic siRNAs. It was expected that biaryl-modified RNAs would be more nuclease resistant than unmodified RNAs. First, the susceptibility of the ONs to snake venom phosphodiesterase (SVPD), a 3′-exonuclease, was examined. Unmodified ON53 and modified ON54, which were labeled at the 5′-ends with fluorescein, were incubated with SVPD. The reactions were analyzed using PAGE under denaturing conditions. As shown in Figure 5a, unmodified ON53 was hydrolyzed randomly after
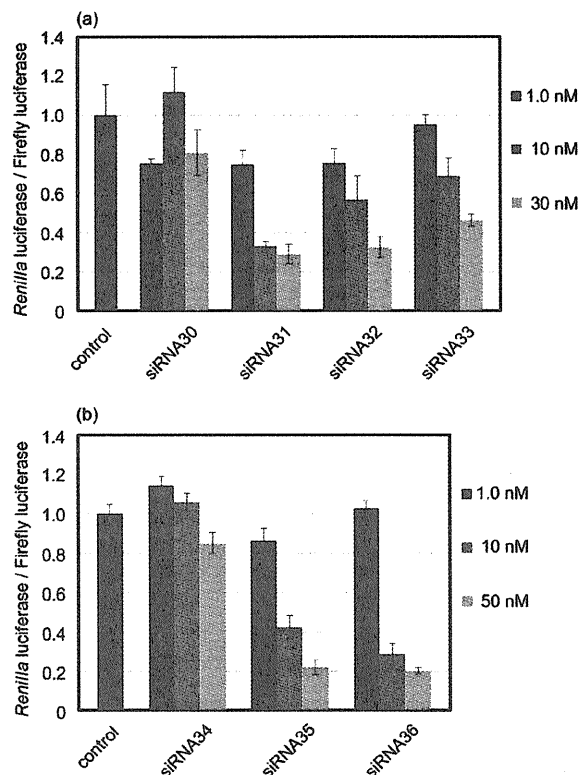

Figure 4. Dual-luciferase assay (3). The experimental conditions are as given in the Experimental Section.
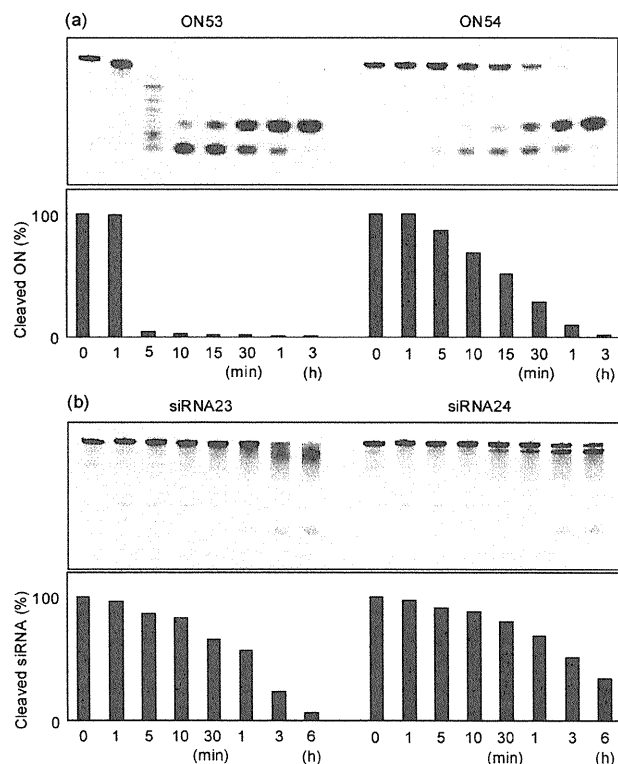

Figure 5. (a) 20% PAGE of 5′-fluorescein-labeled ONs hydrolyzed by SVPD. (b) 20% PAGE of 5′-fluorescein-labeled siRNAs incubated in PBS containing 40% bovine serum. The experimental conditions are as described in the Experimental Section.

5 min of incubation, while modified ON54 was resistant to the enzyme. The half-life ($t_{1/2}$) of unmodified ON53 was less than
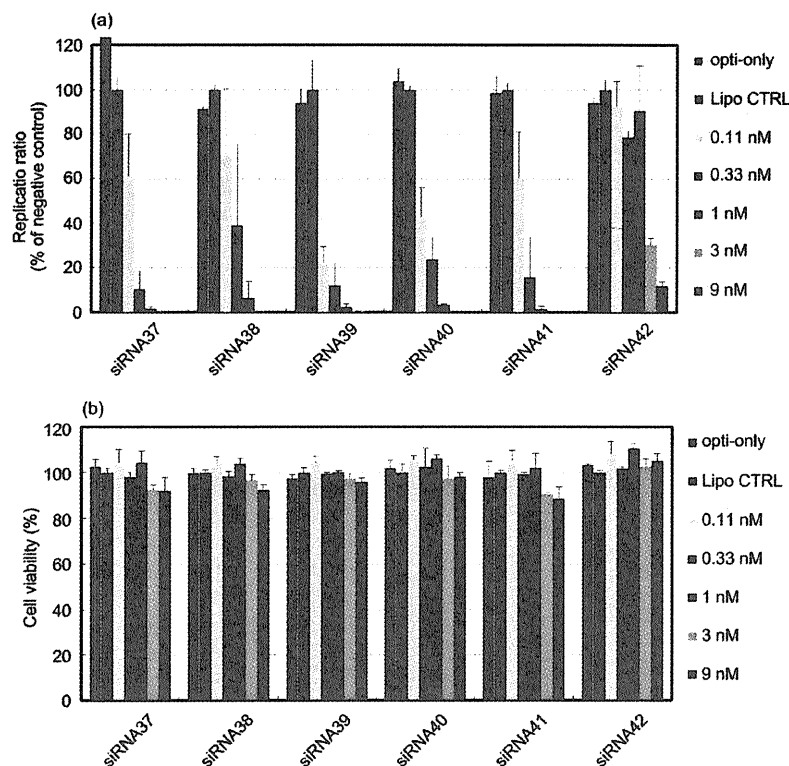
Figure 6. Effect of siRNAs on HCV replication. (a) Inhibition of HCV replication by siRNAs in R6FLR-N replicon cells. HCV replication was calculated by measuring the luminescence ratio with a Bright-Glo luciferase assay system. (b) Cell viability was determined by a WST-8 assay. Data are represented as mean (SD) ($n = 3$). The experimental conditions are as described in the Experimental Section.

5 min, whereas that of the modified ON54 was 17 min. ON54 carrying B^b at its 3′-end was significantly more resistant to SVPD than unmodified ON53.

Next, the stability of siRNAs in PBS containing bovine serum was investigated. Unmodified siRNA23 and modified siRNA24, which were fluorescein-labeled at the 5′ ends of sense strands, were incubated in PBS containing 40% bovine serum. The reactions were analyzed with PAGE under nondenaturing conditions. Figure 5b shows the results. After 6 h of incubation, the band corresponding to the modified siRNA24 duplex was observed, while that corresponding to the unmodified siRNA23 duplex was not observed. Thus, the biaryl-modified siRNA24 is more stable in PBS containing bovine serum than the unmodified siRNA23.

Inhibition of HCV Replication. The genome of hepatitis C virus (HCV) is encoded in an approximately 9.6 kb single-stranded RNA. Previously, we have shown that HCV replication is efficiently suppressed by siRNA38 carrying a benzene-phosphate backbone at its 3′-overhang region (*22*). To assess the efficacy of biaryl-modified siRNAs, we compared the HCV replication-suppressing abilities of modified siRNAs with those of unmodified siRNAs. HCV replication is efficiently suppressed by siRNA targeted to an internal ribosome entry site (IRES) region (*30*), which was chosen as the target for this study. siRNA38, **39**, **40**, and **41** contain B or B^n at the 5′ or 3′ ends of sense and antisense strands. siRNA42 carries 4 mismatched bases in its sequence.

Figure 6 shows the results. The modified siRNAs, **38–41**, exhibited dose-dependent inhibition of HCV replication. They almost completely suppressed HCV replication at a concentration of 1 nM, while the replication ratio of siRNA42, which contained the mismatched bases, was 75% at the same concentration (Figure 6a). The siRNAs exerted no cytotoxic effect at 9 nM (Figure 6b). Thus, it was found that the modified siRNAs **38–41** suppressed HCV replication in a sequence-specific

manner. At 0.11 nM, siRNA39, which carries the naphthalene type of biaryl unit, B^n, at the 5′ and 3′ ends of sense and antisense strands, was the most potent. Thus, B^n modification also effectively improves the silencing activity of siRNAs targeting HCV.

In conclusion, we have demonstrated the synthesis of siRNAs modified with biaryl units. It was found that incorporation of the naphthalene biaryl unit, B^n, at the 5′ and 3′ ends of sense and antisense strands of siRNA improves silencing activity and nuclease resistance. Further, it was revealed that the modified siRNA suppressed HCV replication more efficiently than unmodified siRNA. Thus, the B^n modification may hold promise as a method for improvement of the silencing activity and nuclease-resistance of siRNAs. Recently, it has been reported that lipophilic conjugates of oligonucleotides stimulate nonspecific immune response (*31*). The effects of the biaryl modifications of siRNAs on immune response are now under investigation.

EXPERIMENTAL SECTION

General Remarks. The NMR spectra were recorded at 400 MHz (^{1}H) and 100 MHz (^{13}C) and were reported in ppm downfield from tetramethylsilane. The coupling constants (J) are expressed in Hertz. Thin-layer chromatography was carried out on Merck coated plates $60F_{254}$. Silica gel column chromatography was carried out on Wakogel C-300.

1-[3,5-Bis(hydroxymethyl)phenyl]benzene (2). A solution of 3,5-bis(*tert*-butyldimethylsilyloxymethyl)phenylboronic acid (1.00 g, 2.44 mmol) (*21*) in THF/H₂O (5:1, 12 mL) was added to a solution of 1-iodobenzene (0.50 g, 2.44 mmol) and PdCl₂(dppf)· CH₂Cl₂ (dppf is 1,1′-bis(diphenylphosphanyl)ferrocene) (0.089 g, 0.122 mmol) in THF/H₂O (5:1, 12 mL). 2 M NaOH (3.66 mL) was added to the mixture, and the whole was stirred at 65 °C for 24 h. The reaction mixture was filtered through Celite pad. The eluant was partitioned between EtOAc and H₂O. The

organic layer was washed with aqueous NaHCO₃ (saturated) and brine, dried (Na₂SO₄), and concentrated. The residue was dissolved in THF (12.2 mL). TBAF (1 M in THF, 7.3 mL) was added to the solution, and the mixture was stirred at room temperature for 2 h. The solvent was evaporated in vacuo, and the resulting residue was purified by column chromatography (SiO₂, 2% MeOH in CHCl₃) to give **2** (0.486 g, 93%): ¹H NMR (CDCl₃) δ 7.61−7.34 (m, 8H), 4.77 (s, 4H), 1.84 (s, 2H). ¹³C NMR (DMSO-d_6) δ 133.9, 133.2, 132.9, 120.3, 118.8, 118.5, 116.0, 116.0, 55.7. Anal. Calcd for C₁₄H₁₄O₂: C, 78.48; H, 6.59. Found: C, 78.29; H, 6.46.

1-[3-(4,4′-Dimethoxytrityloxymethyl)-5-(hydroxymethyl)phenyl]benzene (10). A mixture of **2** (0.48 g, 2.24 mmol) and DMTrCl (0.76 g, 2.24 mmol) in pyridine (11 mL) was stirred at room temperature for 4 h. The mixture was partitioned between EtOAc and aqueous NaHCO₃ (saturated). The organic layer was washed with brine, dried (Na₂SO₄), and concentrated. The residue was purified by column chromatography (SiO₂, 15−45% EtOAc in hexane) to give **10** (0.601 g, 52%): ¹H NMR (CDCl₃) δ 7.61−7.21 (m, 17H), 6.87−6.83 (m, 4H), 4.77 (d, 2H, J = 5.6), 4.25 (s, 2H), 3.79 (m, 6H). ¹³C NMR (CDCl₃) δ 158.5, 145.0, 141.5. 141.4, 141.0, 140.2, 136.2, 130.1, 128.7, 128.2, 127.8, 127.3, 127.2, 126.7, 125.1, 124.6, 124.5, 113.1, 86.5, 65.6, 65.4, 60.4, 55.2. Anal. Calcd for C₃₅H₃₄O₅·H₂O: C, 78.63; H, 6.41. Found: C, 78.64; H, 6.16.

1-[3-[[(2-Cyanoethoxy)(N,N-diisopropylamino)phosphanyl]-oxymethyl]-5-(4,4′-dimethoxytrityloxymethyl)phenyl]benzene (11). A mixture of **10** (0.42 g, 0.82 mmol), N,N-diisopropylethylamine (0.71 mL, 4.10 mmol), and chloro(2-cyanoethoxy)(N,N-diisopropylamino)phosphane (0.39 mL, 1.64 mmol) in THF (8 mL) was stirred at room temperature for 1 h. The mixture was partitioned between CHCl₃ and aqueous NaHCO₃ (saturated). The organic layer was washed with brine, dried (Na₂SO₄), and concentrated. The residue was purified by column chromatography (a neutralized SiO₂, EtOAc) to give **11** (0.52 g, 88%): ³¹P NMR (CDCl₃) δ 149.0.

1-[3,5-Bis(hydroxymethyl)phenyl]phenanthrene (4). A solution of **7** in THF/H₂O (5:1, 12 mL) was added to a solution of 9-iodophenanthrene (0.74 g, 2.44 mmol) and PdCl₂(dppf)·CH₂Cl₂ (0.089 g, 0.122 mmol) in THF/H₂O (5:1, 12 mL). 2 M NaOH (3.66 mL) was added to the mixture, and the whole was stirred at 65 °C for 24 h. The reaction mixture was filtered through a Celite pad. The eluant was partitioned between EtOAc and H₂O. The organic layer was washed with aqueous NaHCO₃ (saturated) and brine, dried (Na₂SO₄), and concentrated. The residue was dissolved in THF (12.2 mL). TBAF (1 M in THF, 7.3 mL) was added to the solution, and the mixture was stirred at room temperature for 2 h. The solvent was evaporated in vacuo, and the resulting residue was purified by column chromatography (SiO₂, 2% MeOH in CHCl₃) to give **4** (0.47 g, 60%): ¹H NMR (CDCl₃) δ 8.76 (dd, 2H, J = 8.0 and 21.2), 7.89−7.87 (m, 2H), 7.70−7.48 (m, 8H), 4.82 (s, 4H), 1.80 (s, 2H). ¹³C NMR (CDCl₃) δ 141.3, 140.9, 138.4, 131.4, 130.9, 130.5, 129.8, 128.5, 127.6, 127.3, 126.7, 126.6, 126.5, 126.4, 126.3, 124.4, 122.8, 122.4, 64.5. Anal. Calcd for C₂₂H₁₈O₂·1/5H₂O: C, 83.10; H, 5.83. Found: C, 83.14; H, 5.86.

1-[3-(4,4′-Dimethoxytrityloxymethyl)-5-(hydroxymethyl)phenyl]phenanthrene (15). A mixture of **4** (0.46 g, 1.46 mmol) and DMTrCl (0.50 g, 1.46 mmol) in pyridine (7 mL) was stirred at room temperature for 3 h. The mixture was partitioned between EtOAc and aqueous NaHCO₃ (saturated). The organic layer was washed with brine, dried (Na₂SO₄), and concentrated. The residue was purified by column chromatography (SiO₂, 15−45% EtOAc in hexane) to give **15** (0.55 g, 61%): ¹H NMR (CDCl₃) δ 8.76 (dd, 2H, J = 8.0 and 22.0), 7.96−7.89 (m, 2H), 7.70−7.19 (m, 17H), 6.84−6.81 (m, 4H), 4.81 (s, 2H), 4.29 (s, 2H), 3.78 (m, 6H). ¹³C NMR (CDCl₃) δ 158.4, 145.0, 141.0,

139.8, 138.5, 136.2, 131.5, 131.0, 130.6, 130.1, 129.9, 128.6, 128.2, 128.1, 127.8, 127.5, 127.4, 126.9, 126.8, 126.7, 126.6, 126.5, 126.4, 124.7, 122.9, 122.5, 113.1, 86.5, 65.6, 65.4, 55.2. Anal. Calcd for C₄₃H₃₆O₄·7/10H₂O: C, 82.06; H, 5.99. Found: C, 82.04; H, 6.18.

1-[3-[[(2-Cyanoethoxy)(N,N-diisopropylamino)phosphanyl]oxy-methyl]-5-(4,4′-dimethoxytrityloxymethyl)phenyl]phenanthrene (16). A mixture of **15** (0.35 g, 0.56 mmol), N,N-diisopropylethylamine (0.49 mL, 2.80 mmol), and chloro(2-cyanoethoxy)(N,N-diisopropylamino)phosphane (0.26 mL, 1.12 mmol) in THF (7 mL) was stirred at room temperature for 1 h. The mixture was partitioned between CHCl₃ and aqueous NaHCO₃ (saturated). The organic layer was washed with brine, dried (Na₂SO₄), and concentrated. The residue was purified by column chromatography (a neutralized SiO₂, EtOAc) to give **16** (0.34 g, 74%): ³¹P NMR (CDCl₃) δ 149.0.

Solid Support Synthesis. A mixture of **10** (0.26 g, 0.50 mmol), succinic anhydride (0.15 g, 1.49 mmol), and DMAP (12 mg, 0.10 mmol) in pyridine (5 mL) was stirred at room temperature. After 24 h, the solution was partitioned between CHCl₃ and H₂O, and the organic layer was washed with H₂O and brine. The separated organic phase was dried (Na₂SO₄) and concentrated to give a succinate. Aminopropyl controlled pore glass (1.03 g, 0.12 mmol) was added to a solution of the succinate and EDCI (95 mg, 0.50 mmol) in DMF (12 mL), and the mixture was kept for 48 h at room temperature. After the resin was washed with pyridine, a capping solution (15 mL, 0.1 M DMAP in pyridine/Ac₂O = 9:1, v/v) was added and the whole mixture was kept for 24 h at room temperature. The resin was washed with MeOH and acetone, and dried in vacuo. The amount of loaded compound **10** to solid support was 49 µmol/g from calculation of released dimethoxytrityl cation by a solution of 70% HClO₄/EtOH (3:2, v/v). In a similar manner, solid support with **15** was obtained in 45 µmol/g loading amount.

RNA Synthesis. Synthesis was carried out with a DNA/RNA synthesizer by phosphoramidite method. Deprotection of bases and phosphates was performed in concentrated NH₄OH/EtOH (3:1, v/v) at room temperature for 12 h. 2′-TBDMS groups were removed by 1.0 M tetrabutylammonium fluoride (TBAF, Aldrich) in THF at room temperature for 12 h. The reaction was quenched with 0.1 M TEAA buffer (pH 7.0) and desalted on a Sep-Pak C18 cartridge. Deprotected ONs were purified by 20% PAGE containing 7 M urea to give the highly purified ON45 (23), ON46 (21), ON47 (27), ON48 (35), ON49 (28), ON50 (36), ON51 (24), ON52 (17), ON53 (20), ON54 (45), ON57 (12), ON58 (31), ON59 (16), ON60 (19), ON63 (30), ON64 (25), ON65 (11), ON66 (23), ON69 (26), ON70 (28), ON71 (13), ON74 (38), ON75 (38), ON76 (16), ON77 (24), ON78 (17), ON79 (26). The yields are indicated in parentheses as OD units at 260 nm starting from 1.0 µmol scale. Extinction coefficients of the ONs were calculated from those of mono-nucleotides and dinucleotides according to the nearest-neighbor approximation method (*32*).

MALDI-TOF/MS Analysis of RNAs. Spectra were obtained with a time-of-flight mass spectrometer. ON45: calculated mass, 6443.9; observed mass, 6449.2. ON46: calculated mass, 6753.0; observed mass, 6751.8. ON47: calculated mass, 6543.9; observed mass, 6547.9. ON48: calculated mass, 6853.0; observed mass, 6853.2. ON49: calculated mass, 6644.0; observed mass, 6646.4. ON50: calculated mass, 6953.1; observed mass, 6951.0. ON51: calculated mass, 6696.0; observed mass, 6693.1. ON52: calculated mass, 7005.1; observed mass, 7004.8. ON53: calculated mass, 7067.0; observed mass, 7065.5. ON54: calculated mass, 7011.0; observed mass, 7007.9. ON57: calculated mass, 6859.2; observed mass, 6852.0. ON58: calculated mass, 6909.0; observed mass, 6902.4. ON59: calculated mass, 7008.3; observed mass, 7004.9. ON60: calculated mass, 7058.4; observed

mass, 7052.4. ON63: calculated mass, 6641.9; observed mass, 6645.5. ON64: calculated mass, 6688.0; observed mass, 6685.9. ON65: calculated mass, 6814.0; observed mass, 6820.1. ON66: calculated mass, 6522.9; observed mass, 6526.2. ON69: calculated mass, 6745.9; observed mass, 6746.1. ON70: calculated mass, 6568.9; observed mass, 6565.5. ON71: calculated mass, 6695.0; observed mass, 6696.0. ON74: calculated mass, 6739.9; observed mass, 6739.0. ON75: calculated mass, 6802.9; observed mass, 6801.4. ON76: calculated mass, 7066.0; observed mass, 7061.8. ON77: calculated mass, 6929.0; observed mass, 6933.2. ON78: calculated mass, 7066.0; observed mass, 7067.1. ON79: calculated mass, 6929.0; observed mass, 6931.6.

Thermal Denaturation Study. Each solution containing each siRNA (3 μM) in a buffer composed of 10 mM Na_2HPO_4/ NaH_2PO_4 (pH 7.0) and 100 mM NaCl was heated at 95 °C for 3 min, then cooled gradually to an appropriate temperature, and used for the thermal denaturation studies. Thermally induced transitions of each mixture were monitored at 260 nm with a spectrophotometer.

Dual-Luciferase Assay. HeLa cells were grown at 37 °C in a humidified atmosphere of 5% CO_2 in air in Minimum Essential Medium (MEM) (Invitrogen) supplemented with 10% fetal bovine serum (FBS). Twenty-four hours before transfection, HeLa cells (4 × 10^4/mL) were transferred to 96-well plates (100 μL per well). They were transfected, using TransFast (Promega), according to instructions for transfection of adherent cell lines. Cells in each well were transfected with a solution (35 μL) of 20 ng of psiCHECK-2 vector (Promega), the indicated amounts of siRNAs, and 0.3 μg of TransFast in Opti-MEM I Reduced-Serum Medium (Invitrogen), and incubated at 37 °C. Transfection without siRNA was used as a control. After 1 h, MEM (100 μL) containing 10% FBS and antibiotics was added to each well, and the whole was further incubated at 37 °C. After 24 h, cell extracts were prepared in Passive Lysis Buffer (Promega). Activities of firefly and *Renilla* luciferases in cell lysates were determined with a dual-luciferase assay system (Promega) according to a manufacturer's protocol. The results were confirmed by at least three independent transfection experiments with two cultures each and are expressed as the average from four experiments as mean ± SD.

Partial Hydrolysis of ONs with Snake Venom Phosphodiesterase. Each ON (300 pmol) labeled with fluorescein at the 5'-end was incubated with snake venom phosphodiesterase (3 ng) in a buffer containing 37.5 mM Tris-HCl (pH 7.0) and 7.5 mM $MgCl_2$ (total 100 μL) at 37 °C. At appropriate periods, aliquots (5 μL) of the reaction mixture were separated and added to a solution of 9 M urea (15 μL). The mixtures were analyzed by electrophoresis on 20% polyacrylamide gel containing 7 M urea. The labeled ON in the gel was visualized by a Typhoon system (Amersham Biosciences).

Stability of siRNAs in the PBS Containing Bovine Serum. Each siRNA (600 pmol) labeled with fluorescein at the 5'-end of a sense strand was incubated in PBS (300 μL) containing 40% bovine serum at 37 °C. At appropriate periods, aliquots (5 μL) of the reaction mixture were separated and added to a loading solution (15 μL), and then the whole was immediately frozen in dry ice. The mixtures were analyzed by electrophoresis on 20% polyacrylamide gel under nondenaturing conditions. The labeled siRNA in the gel was visualized by a Typhoon system (Amersham Biosciences).

Subgenomic HCV Replicon Cells. Subgenomic HCV replicon cells (R6FLR-N) were conditional expression system of the HCV-nonstructure region and luciferase gene. These cells were cultured in DMEM-GlutaMAX High glucose (GIBCO) supplemented with 10% FBS, 1 unit penicillin (GIBCO), 100 μg/mL streptomycin (GIBCO), and 500 μg/mL G418 (GIBCO).

Transfection and Evaluation of Virus Replication. The subgenomic HCV replicon cells (R6FLR-N) were transfected with the siRNAs by reverse transfection. The cells were plated in 96-well plate (Falcon) at a density of 4 × 10^3 cells/well. Each siRNA (100 aM − 1 nM) was transfected to the cells using Lipofectamine RNAiMAX (Invitrogen) and Opti-MEM (GIBCO-BRL). The cells were incubated for 72 h after being transfected with siRNAs. HCV replication was evaluated by luminescence in a Mithras LB940 (Berthold Technologies, Wildbad, Germany) using Bright-Glo Luciferase Assay System (Promega) according to the manufacturer's protocol.

Cell Viability. In order to evaluate cytotoxic effects of the siRNAs, cell viabilities were measured by metabolic conversion of 2-(2-methoxy-4-nitrophenyl)-3-(4-nitrophenyl)-5-(2,4-disulfophenyl)-2*H*-tetrazolium, monosodium salt (WST-8) using a Cell Counting Kit-8 (Dojindo, Kumamoto, Japan) according to the manufactuer's protocol.

LITERATURE CITED

(1) Fire, A., Xu, S., Montgomery, M. K., Kostas, S. A., Driver, S. E., and Mello, C. C. (1998) Potent and specific genetic interference by double-stranded RNA in *Caenorhabditis elegans*. *Nature 391*, 806–811.

(2) Elbashir, S. M., Harborth, J., Lendeckel, W., Yalcin, A., Weber, K., and Tuschl, T. (2001) Duplexes of 21-nucleotide RNAs mediate RNA interference in cultured mammalian cells. *Nature 411*, 494–498.

(3) Elbashir, S. M., Lendeckel, W., and Tuschl, T. (2001) RNA interference is mediated by 21- and 22nucleotide RNAs. *Genes Dev. 15*, 188–200.

(4) Bumcrot, D., Manoharan, M., Koteliansky, V., and Sah, D. W. Y. (2006) RNAi therapeutics: a potential new class of pharmaceutical drugs. *Nat. Chem. Biol. 2*, 711–719.

(5) Behlke, M. A. (2006) Progress toward *in vivo* use of siRNAs. *Mol. Ther. 13*, 644–670.

(6) Kim, D. A., and Rossi, J. J. (2007) Strategies for silencing human disease using RNA interference. *Nat. Rev. Genet. 8*, 173–184.

(7) Schwarz, D. S., Hutvágner, G., Du, T., Xu, Z., Aronin, N., and Zamore, P. D. (2003) Asymmetry in the assembly of the RNAi enzyme complex. *Cell 115*, 199–208.

(8) Khvorova, A., Reynolds, A., and Jayasena, S. D. (2003) Functional siRNAs and miRNAsexhibit strand bias. *Cell 115*, 209–216.

(9) Tomari, Y., Matranga, C., Haley, B., Martinez, N., and Zamore, P. D. (2004) A protein sensor for siRNA asymmetry. *Science 306*, 1377–1380.

(10) Steiner, F. A., Hoogstrate, S. W., Okihara, K. L., Thijssen, K. L., Ketting, R. F., Plasterk, R. H. A., and Sijen, T. (2007) Structural features of small RNA precursors determine Argonaute loading in *Caenorhabditis elegans*. *Nat. Struct. Mol. Biol. 14*, 927–933.

(11) Mi, S., Cai, T., Hu, Y., Chen, Y., Hodges, E., Ni, F., Wu, L., Li, S., Zhou, H., Long, C., Chen, S., Hannon, G. J., and Qi, Y. (2008) Sorting of small RNAs into *Arabidopsis* Argonate complexes is directed by the 5' terminal nucleotide. *Cell 133*, 116–127.

(12) Kawamata, T., Seitz, H., and Tomari, Y. (2009) Structural determinants of miRNAs for RISC loading and slicer-independent unwinding. *Nat. Struct. Mol. Biol. 16*, 953–960.

(13) Yoda, M., Kawamata, T., Paroo, Z., Ye, X., Iwasaki, S., Liu, Q., and Tomari, Y. (2010) ATP-dependent human RISC assembly pathways. *Nat. Struct. Mol. Biol. 16*, 17–23.

(14) Ghildiyal, M., Xu, J., Seitz, H., Weng, Z., and Zamore, P. D. (2010) Sorting of *Drosophila* small silencing RNAs partitions microRNA* strands into the RNA interference pathway. *RNA 16*, 43–56.

(15) Chen, P. Y., Weinmann, L., Gaidatzis, D., Pei, Y., Zavolan, M., Tuschl, T., and Meister, G. (2008) Strand-specific 5'-O-methylation of siRNA duplexes controls guide strand selection and targeting specificity. *RNA 14*, 263–274.

(16) Parker, J. S., Roe, S. M., and Barford, D. (2005) Structure insights into mRNA recognition from a PIWI domain-siRNA guide complex. *Nature 434*, 663–666.

(17) Ma, J.-B., Yuan, Y.-R., Meister, G., Pei, Y., Tuschl, T., and Patel, D. J. (2005) Structure basis for 5'-end-specific recognition of guide RNA by the *A. fulgidus* Piwi protein. *Nature 434*, 666–670.

(18) Wang, Y., Sheng, G., Juranek, S., Tuschl, T., and Patel, D. J. (2008) Structure of the guide-strand-containing argonaute silencing complex. *Nature 456*, 209–213.

(19) Wang, Y., Juranek, S., Li, H., Sheng, G., Tuschl, T., and Patel, D. J. (2008) Structure of an argonaute silencing complex with a seed-containing guide DNA and target RNA duplex. *Nature 456*, 921–926.

(20) Wang, Y., Juranek, S., Li, H., Sheng, G., Wardle, G. S., Tuschl, T., and Patel, D. J. (2010) Nucleation, propagation and cleavage of target RNAs in Ago silencing complexes. *Nature 461*, 754–761.

(21) Ueno, Y., Komatsuzaki, S., Takasu, K., Kawai, S., Kitamura, Y., and Kitade, Y. (2009) Synthesis and properties of oligonucleotides containing novel fluorescent biaryl units. *Eur. J. Org. Chem. 28*, 4763–4769.

(22) Ueno, Y., Watanabe, Y., Shibata, A., Yoshikawa, K., Takano, T., Kohara, M., and Kitade, Y. (2009) Synthesis of nuclease-resistant siRNAs possessing universal overhangs. *Bioorg. Med. Chem. 17*, 1974–1981.

(23) Lingel, A., Simon, B., Izaurralde, E., and Sattler, M. (2003) Structure and nucleic-acid binding of the *Drosophila* Argonaute 2 PAZ domain. *Nature 426*, 465–469.

(24) Yan, K. S., Yan, S., Farooq, A., Han, A., Zeng, L., and Zhou, M.-M. (2003) Structure and conserved RNA binding of the PAZ domain. *Nature 426*, 469–474.

(25) Song, J.-J., Liu, J., Tolia, N. H., Schneiderman, J., Smith, S. K., Martienssen, R. A., Hannon, G. J., and Joshua-Tor, L. (2003) The crystal structure of the Argonaute2 PAZ domain reveals an RNA binding motif in RNAi effector complexes. *Nat. Struct. Biol. 12*, 1026–1032.

(26) Ma, J.-B., Te, K., and Patel, D. J. (2004) Structure basis for overhang-specific small interfering RNA recognition by the PAZ domain. *Nature 429*, 318–322.

(27) Somoza, Á., Terrazas, M., and Eritja, R. (2010) Modified siRNAs for the study of the PAZ domain. *Chem. Commun. 46*, 4270–4272.

(28) Qiu, S., Adema, C. M., and Lane, T. (2005) A computational study of off-target effects of RNA interference. *Nucleic Acids. Res. 33*, 1834–1847.

(29) Jackson, A. L., Burchard, J., Schelter, J., Chau, B. N., Cleary, M., Lim, L., and Linsley, P. S. (2006) Widespread siRNA "off-target" transcript silencing mediated by seed region sequence complementarity. *RNA 12*, 1179–1187.

(30) Watanabe, T., Sudoh, M., Miyagishi, M., Akashi, H., Arai, M., Inoue, K., Taira, K., Yoshida, M., and Kohara, M. (2006) Intracellular-diced dsRNA has enhanced efficacy for silencing HCV RNA and overcomes variation in the viral genotype. *Gene Ther. 13*, 883–892.

(31) Uhlmann, E., Vollmer, J., and Krieg, A. M. (2010) Nucleic acid-lipophilic conjugates. U.S. Patent Appl. US 20100183639A1.

(32) Puglisi, J. D., and Tinoco, I., Jr. (1989) *In Methods in Enzymology*, Dahlberg, J. E., and Abelson, J. N., Eds.; pp 304–325, Vol 180, Academic Press, Inc., San Diego.

ORIGINAL ARTICLE

Establishment of infectious HCV virion-producing cells with newly designed full-genome replicon RNA

Masaaki Arai · Hidenori Suzuki · Yoshimi Tobita ·
Asako Takagi · Koichi Okamoto · Atsunori Ohta ·
Masayuki Sudoh · Michinori Kohara

Abstract Hepatitis C virus (HCV) replicon systems enable in-depth analysis of the life cycle of HCV. However, the previously reported full-genome replicon system is unable to produce authentic virions. On the basis of these results, we constructed newly designed full-genomic replicon RNA, which is composed of the intact 5′-terminal-half RNA extending to the NS2 region flanked by an extra selection marker gene. Huh-7 cells harboring this full-genomic RNA proliferated well under G418 selection and secreted virion-like particles into the supernatant. These particles, which were round and 50 nm in diameter when analyzed by electron microscopy, had a buoyant density of 1.08 g/mL that shifted to 1.19 g/mL after NP-40 treatment; these figures match the putative densities of intact virions and nucleocapsids without envelope. The particles also showed infectivity in a colony-forming assay. This system may offer another option for investigating the life cycle of HCV.

M. Arai · A. Takagi
Pharmacology Research Laboratories I,
Mitsubishi Tanabe Pharma Corporation,
1000, Kamoshida-cho, Aoba-ku, Yokohama 227-0033, Japan

M. Arai · Y. Tobita · M. Kohara (✉)
Infectious Diseases Project, The Tokyo Metropolitan Institute
of Medical Science, 1-6, Kamikitazawa, 2-chome,
Setagaya-ku, Tokyo 156-8506, Japan
e-mail: kohara-mc@igakuken.or.jp

H. Suzuki
Laboratory for Electron Microscopy, Tokyo Metropolitan
Institute of Medical Science, 1-6, Kamikitazawa, 2-chome,
Setagaya-ku, Tokyo 156-8506, Japan

K. Okamoto · A. Ohta · M. Sudoh
Kamakura Research Laboratories, Chugai Pharmaceutical Co.,
Ltd., 200 Kajiwara, Kamakura, Kanagawa 247-8530, Japan

Introduction

Hepatitis C virus (HCV) is a major cause of chronic hepatitis, liver cirrhosis, and hepatocellular carcinoma. With over 170 million people currently infected [2], HCV is a growing public-health burden.

The life cycle of HCV has been difficult to study because cell culture and small animal models of HCV infection are not available. The recent development of HCV replicon systems has permitted the study of HCV translation and RNA replication in human hepatoma-derived Huh-7 cells in vitro [17]. However, these replicon systems cannot produce authentic virions because they lack the infection steps, and analysis of these infection steps is very important for understanding HCV pathogenesis.

Recently, some groups have successfully established in vitro infection systems [16, 21, 26, 28–30]. The strategies of these systems are basically the same as the ones used for transfection of Huh-7 cells or their derivatives with in vitro-generated HCV genome RNA [1]. The non-structural regions used in those studies were from the 2a genotype JFH (Japan Fulminant Hepatitis)-1 clone or the 1a genotype H77 clone. The former is known for its exceptionally vigorous amplification and broad permissiveness in cultured cells other than Huh-7 [3, 12, 13], while the latter shows only poor replication ability. Another group reported a newly established immortalized hepatocyte cell line that is susceptible to HCV infection, but only modest improvement was achieved [10]. There are also reports of a system using a full-genome replicon that has the entire coding region under the control of the internal ribosomal entry site of encephalomyocarditis virus, EMCV-IRES; however, this system also failed to show infectivity in the G418 selection assay [7, 20], and secretion of particles with the putative characteristics of HCV virions could not be confirmed [4].

🖄 Springer

We now report the establishment of infectious virion-producing replicon cells that utilize an ordinary genotype 1b replicon strain. In order to address the contribution of structural and non-structural gene products to the maturation of HCV particles in vitro, we partitioned these regions in the same cistron of the full genomic sequence, thereby enabling the functions of these structural and non-structural genes to be studied separately. Thus, we termed this construction "divided open reading frame carrying" full genome replicon, or dORF replicon.

Virus particles secreted from cells containing dORF replicon RNA, as confirmed morphologically using electron microscopy, were shown to be able to infect Huh-7 cells. Replication of dORF replicon RNA was so efficient that infected cells could survive and proliferate under G418 selection to form colonies, as seen after transfection with replicon RNA. In addition, a reporter gene was successfully inserted into the construct, and activity of the reporter gene could be transmitted to naive Huh-7 cells by infection.

We believe that the success of this system is due to the difference in the construction of the replicon, namely, having the intact 5′ half extending to NS2 instead of being divided at the beginning of the core region. Although further investigation is required to elucidate whether the encapsidation signal of HCV is located in the region that is divided in the full-genome replicon, this is the first report to describe genome-length replicon-containing cells that can produce virus particles that have the putative characteristics of the HCV virion, in terms of both morphology and biological properties.

Results

dORF replicon RNA can replicate in Huh-7 cells

We began this study with transfection with the dORF replicon RNAs (Fig. 1A). When 30 μg of each RNA was electroporated into 4×10^6 Huh-7 cells, the dORF and dORF bla RNA-transfected cells formed 20 and 5 colonies, respectively, after 3 weeks of G418 selection. No colonies appeared as a result of transfection with polymerase-defective mutants (data not shown). Two colonies were picked, amplified, and designated as dORF replicon cell #1 and #2, and dORF bla replicon cell #1 and #2. Some of these cells were then used for quantification of HCV RNA and northern blot analysis (Fig. 1B). Northern blot analysis showed that these clones contained HCV RNAs of the expected size and that the HCV RNA copy numbers of these clones did not differ substantially from that of the subgenomic replicon, indicating that replication ability had not been hampered by insertion of the structural genes, which is counter to what was expected. Western blot

analysis showed that these clones express both structural and non-structural proteins (Fig. 1C). These results confirmed that transfected dORF HCV RNAs can replicate in Huh-7 cells, just as authentic subgenomic replicon RNAs do.

dORF replicon cells secrete virus particles

In a previous study, HCV subgenomic replicon cells secreted RNase-resistant subgenomic RNA into the culture supernatant [4, 7, 20]. We also detected a similar amount of RNase-resistant HCV RNA in the culture supernatant of our dORF replicon cells, as well as of the subgenomic and full-genome replicon cells. These supernatants showed no significant differences in terms of distribution of HCV RNA in buoyant density gradient analysis (Figs. 2A, B, open square). In contrast, there was a clear difference between these supernatants after NP-40 treatment. While almost all of the HCV RNA in the supernatant of the subgenomic replicon cells was eliminated by NP-40 treatment (Fig. 2A, filled triangle), there remained a peak of HCV RNA at a density of 1.18 g/mL in the supernatant of the dORF replicon cells (Fig. 2B, filled triangle). These results were confirmed in the same experiment, using concentrated culture supernatant (Figs. 2C, D). We also confirmed the results of previous reports [7, 20], which showed no genomic RNA resistant to NP-40 treatment in the supernatant of full-genome replicon cells (Fig. 2E). Secreted core proteins in the concentrated supernatant showed a different density gradient distribution compared to genomic RNA (Fig. 2F, open circle) in that the core proteins were present at densities of 1.1–1.2 g/mL, while HCV RNA was more broadly distributed in the range of 1.06–1.22 g/mL. Thus, HCV RNA and core proteins were not always associated with each other. However, after NP-40 treatment, core proteins were found only in the same fraction as HCV RNA, at 1.19 g/mL (Fig. 2F, filled triangle). Taken together with the results of the report mentioned above [20], our replicon cells harboring dORF RNA appeared to secrete particles with core proteins that were assembled into nucleocapsids as well as particles without core proteins that were sensitive to NP-40 treatment, like the ones from subgenomic and full-genome replicon cells. We concluded that the broader distribution of the HCV genome RNA in the density gradient than that of the core protein was caused by the overlapping distribution of these two particle types, and that the remaining peaks of genome RNA and core protein after NP-40 treatment were of nucleocapsids that had had their envelopes stripped off by NP-40 [11].

According to our hypothesis, the distribution of core proteins in the density gradient represented that of the

Fig. 1 Confirmation of
"divided open reading frame
carrying" (dORF) replicon
cells. (A) Schematic
representations of replicon
RNAs used in this study. All the
replicon constructs contained
inserts just after the T7
promotor. UTR, untranslated
region; NS, non-structural
protein; neo, neomycin
phosphotransferase II; EMCV,
encephalomyocarditis virus;
IRES, internal ribosomal entry
site; FMDV, foot-and-mouth
disease virus; bla, beta-
lactamase. (B) Northern blot
analysis. A 10-µg amount of
total RNA from each cell
sample was loaded. Subgenomic
replicon RNA: 10^8 copies of in
vitro-generated subgenomic
RNA. Numbers below the lanes
are the HCV copy number per
microgram of total RNA. Huh-7
cell, subgenomic replicon cell,
dORF replicon cell #1, #2,
dORF bla replicon cell #1, #2.
(C) Western blot analysis. A
10-µg amount of each cell lysate
was loaded. Huh-7 cell, Huh-7-
JFH1: Huh-7 cell transfected
with JFH1 viral RNA,
subgenomic replicon cell, full-
genome replicon cell, dORF
replicon cell #1, #2, dORF bla
replicon cell #1, #2
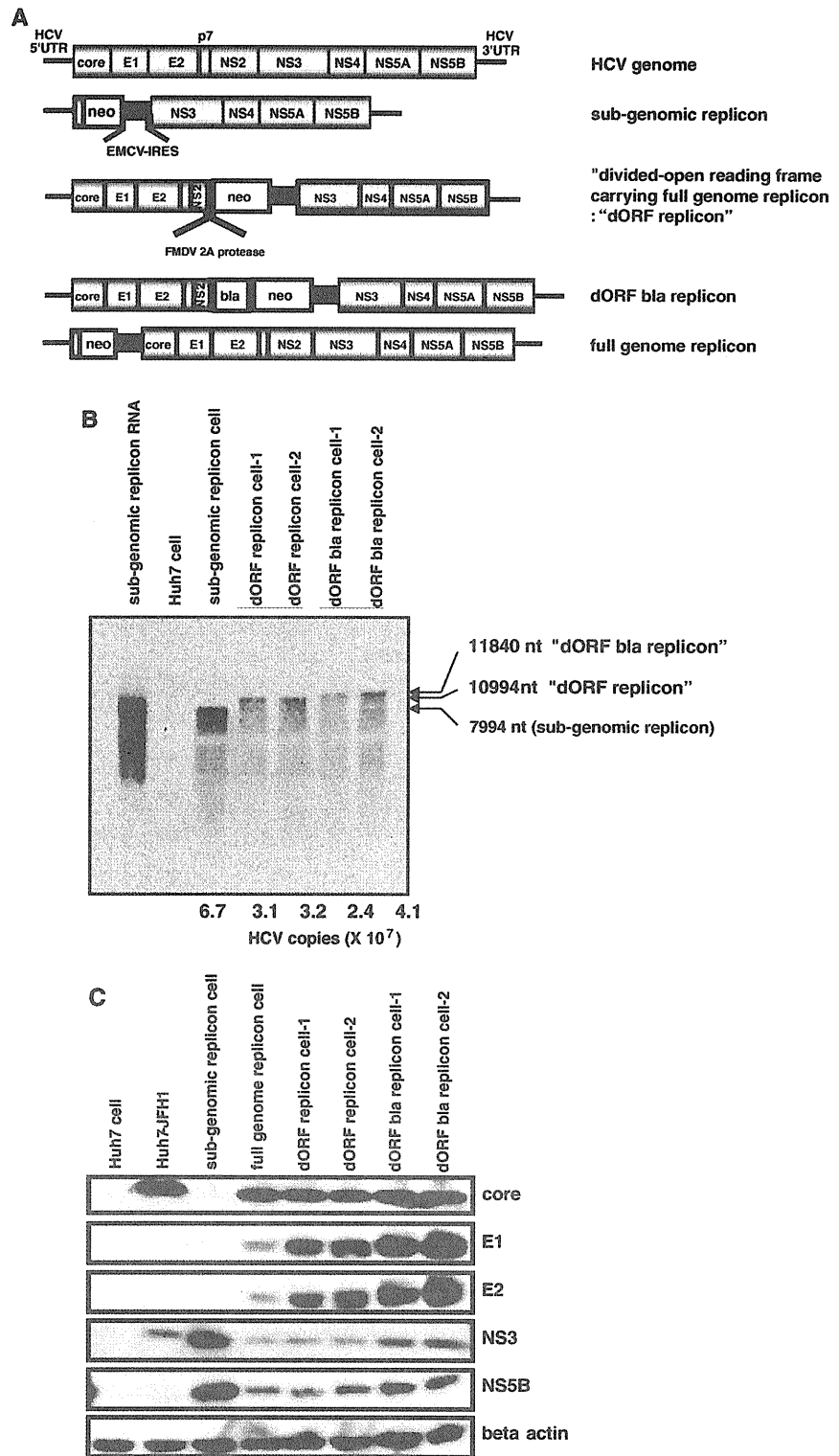
intact virion, and we therefore tried to observe virions
directly by electron microscopy, using the fraction in which
the core protein was present. We easily identified numerous
round-shaped virus particles approximately 50 nm in
diameter by scanning electron microscopy (Fig. 3A). Fur-
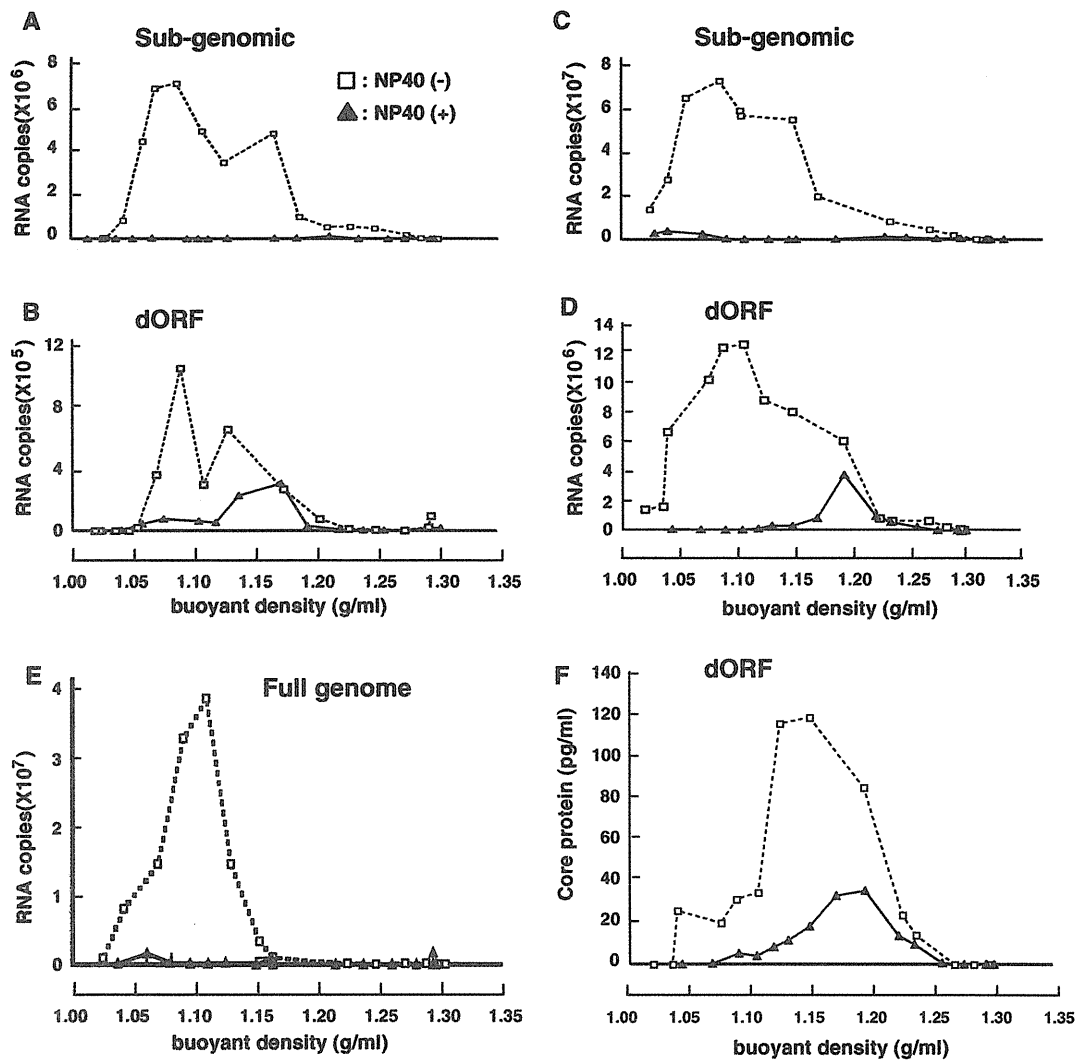thermore, when the immunogold method using anti-E2

Fig. 2 Density gradient analysis of supernatants. Culture supernatants were treated with RNaseA and loaded directly onto a sucrose density gradient without treatment (open square) or after NP-40 treatment (filled triangle). Quantification of HCV RNA in each fraction of supernatant from the subgenomic replicon (A) and dORF

replicon (B). Analysis of concentrated culture supernatant from the subgenomic replicon (C) and dORF replicon (D). Concentrated culture supernatant from the full-genome replicon NNC#2 was also analyzed (E). Quantification of HCV core protein in each fraction of supernatant from the dORF replicon (F)

RR6 antibody was applied to samples fixed on the mesh, transmission electron microscopy could be used to visualize virus particles labeled with colloidal gold (Fig. 3B). These findings provide evidence of intact virion production from our dORF replicon cells.

Secreted virus particles can infect naive Huh-7 cells

Next, we examined the infectivity of these virus particles. The culture supernatants of these dORF replicon cells were collected, and 3 kinds of naive Huh-7 cells, one purchased

from the J.C.R.B. (Japanese Collection of Research Bioresources) and the other two, designated as the cured cells F2 and K4, generated by IFN-α treatment of 1bneo/delS replicon cells, were infected with these supernatants. After two sequential passages and three weeks of G418 selection as described above, a number of colonies appeared, as shown in Fig. 4A. The largest number of colonies was produced from the cured cells K4, and slightly fewer colonies were produced from the cured cells F2, while no colonies appeared when normal Huh-7 cells were used (data not shown). The same infection experiment carried
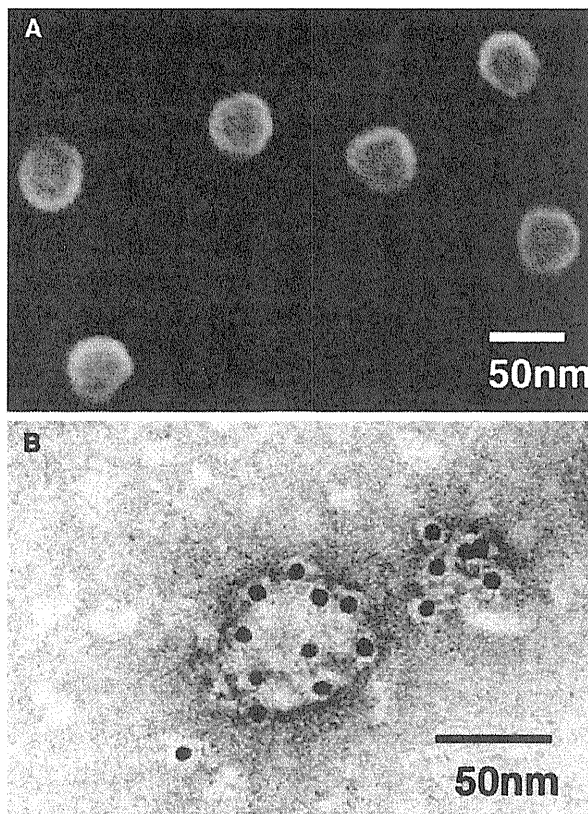
Fig. 3 Electron microscopy analysis of virus-like particles. The core-protein-rich fraction collected from the density gradient was further concentrated by ultracentrifugation and observed by scanning electron microscopy (A). The same fraction attached to formvar-coated grids was incubated with rabbit anti-E2 RR6 antibody, treated with goat anti-rabbit IgG coupled to 10-nm colloidal gold, negatively stained with uranyl acetate, and then examined by transmission electron microscopy (B)

out with full-genome replicon cells produced no infectivity in the supernatant (data not shown). Under the most efficient conditions, the titer of the supernatant reached as high as 20 cfu (colony-forming units) per milliliter when the putative doubling time of these cells was approximately 24 h. Furthermore, the appearance of colonies was abolished by addition of the antibody JS-81 (BD Pharmingen), an antibody to CD81, a possible co-receptor of HCV [22] (Fig. 4B).

Next, we propagated some of these colonies for further analysis. Northern blot analysis showed that these clones carry HCV RNAs of reasonable size (Fig. 5A), including subgenomic RNA (7994 bases), dORF RNA (10994 bases), and dORF bla RNA (11840 bases). Western blot analysis revealed that the cell clones that were infected with supernatant from Huh-7 cells containing the dORF replicon expressed structural proteins (Fig. 5B), indicating that the

colonies were not just the reappearance of subgenomic replicons hidden in the cured cells.

Together, our findings indicate that these particles in the supernatant infected the Huh-7 cells through a CD81-associated pathway and that infected cells formed colonies after G418 selection, similar to what was observed with electroporation with subgenomic RNA.

A reporter gene inserted into the dORF replicon RNA can be transmitted through infection
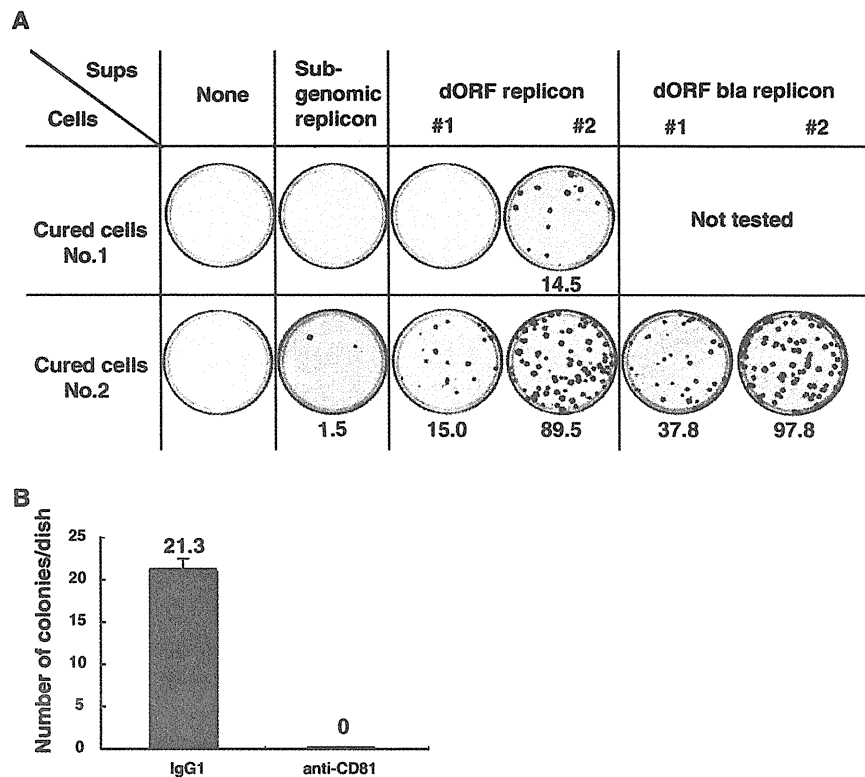
First, we confirmed that the beta-lactamase gene in the dORF bla replicon RNA was active in established replicon cell clones and able to process the green fluorescent substrate into blue fluorescent product (Fig. 6A). Next, we attempted to detect the activity of the beta-lactamase gene in the cloned infected colonies. Three clones grown from cells infected with the dORF bla supernatant were treated using a GeneBLAzer In Vivo Detection Kit. One clone was positive for blue fluorescence (Fig. 6B), demonstrating that a reporter gene inserted into the dORF replicon could be transmitted to naive Huh-7 cells through secreted virus particles in the culture supernatant.

Discussion

There have been several previous reports of full-genome HCV replicons that can replicate well in Huh-7 cells and express sufficient amounts of structural proteins [1, 4, 7, 14, 20]. Pietschmann et al. (2002) observed the secretion of an RNase-resistant HCV genome into the supernatant from both full-genome and subgenomic replicon cells and non-specific uptake of these genomes by naive Huh-7 cells. Ikeda et al. (2002) were also unable to detect any infectivity in the supernatant of their full-genome replicon cells. They assumed that the reason for this failure was the inability of Huh-7 cells to release intact virions or to be infected by the virus, although this was later demonstrated not to be the case by a series of reports on infection using the JFH-1 clone [16, 26, 30].

First, we attempted to improve the efficiency of the full-genome replicon in two ways, namely, by modifying the construct and reducing the genome size. Numerous studies have examined the encapsidation signal in the genomic RNA of positive-sense single-stranded viruses [5, 8, 9]. Frolova et al. [5] showed that the encapsidation signal of Sindbis virus lies in the nsP1 gene and is 132 nucleotides long. Johansen et al. [9] found that the IRES of poliovirus had the ability to enhance the efficiency of packaging of the polio subgenomic replicon. We think that these findings indicate that the construction of the genome could affect the efficacy of encapsidation, and we therefore decided to

Fig. 4 Infectivity of supernatants from various replicon cells. Colonies of cells infected with the indicated supernatant. Numbers shown below the plates are the average of a total of four plates per condition (A). Inhibition of infection by anti-CD81 antibody. Cured cell K4 cells (No.2 in Fig. 4A) were treated with mouse IgG1 as the negative control or anti-CD81 before infection (B)

A

Sups \ Cells	None	Sub-genomic replicon	dORF replicon #1	dORF replicon #2	dORF bla replicon #1	dORF bla replicon #2
Cured cells No.1				14.5	Not tested	
Cured cells No.2		1.5	15.0	89.5	37.8	97.8

B

change the site of genome division from the beginning of the core region to the middle of the NS2 region. Regarding the size of the genome, there have been reports that the insertion of a foreign gene of significant size can result in the deletion of a portion of the chimeric genome during replication [18, 19]. We therefore removed the second half of the NS2 region, because this region appears to be unnecessary for both replication and packaging in Huh-7 cells, and this deletion was found to have no influence on the efficacy of encapsidation, as there were no apparent differences between the NS2-deleted construct and the one containing the entire NS2 region (data not shown).

Our established dORF replicon was able to replicate well in Huh-7 cells and express sufficient amounts of structural proteins, similar to the previously reported full-genome replicon. Although both the dORF replicon cells and the previously reported full-genome replicons secreted RNase-resistant genomes, there was a striking difference between these two full-genome replicons when NP-40 treatment was carried out on their supernatants. There was no RNase-resistant genome left in the NP-40-treated supernatant of full-genome replicons, although density gradient analysis of the NP-40-treated supernatant of dORF replicon cells clearly showed the coexistence of the HCV genome and core proteins at a peak of 1.18 g/mL. This peak may represent NP-40-resistant nucleocapsids. The

distribution of core proteins in the density gradient analysis of the concentrated supernatant of the dORF replicons did not match that of the HCV genome. A reasonable explanation for this mismatch is that the lighter side of the broad peak of the HCV genome was not representative of intact virions and is instead an indication of secretion by a pathway used in subgenomic replicon cells, which differs from the natural process. The fact that the peak of the HCV genome of full-genome replicons was located in a narrow range on the lighter side compared to that of the dORF replicons supports this hypothesis. We observed round particles in the concentrated core protein fraction using electron microscopy, and those particles also seemed to contain core proteins. These findings indicate that our dORF replicon cells produced both intact virions and artificial membranous particles, with the former having the morphological and biophysical characteristics of putative virions.

The colony-forming assay clearly demonstrated the ability of the supernatants of our dORF replicon cells to infect Huh-7 cells efficiently. The reason for the difference in efficacy between the two cured cells is uncertain but may involve the ability to support replication or the level of receptor expression. This needs to be clarified in order to improve the efficiency of HCV infection in vitro. Differences in the efficiency of infection were also noted between

A
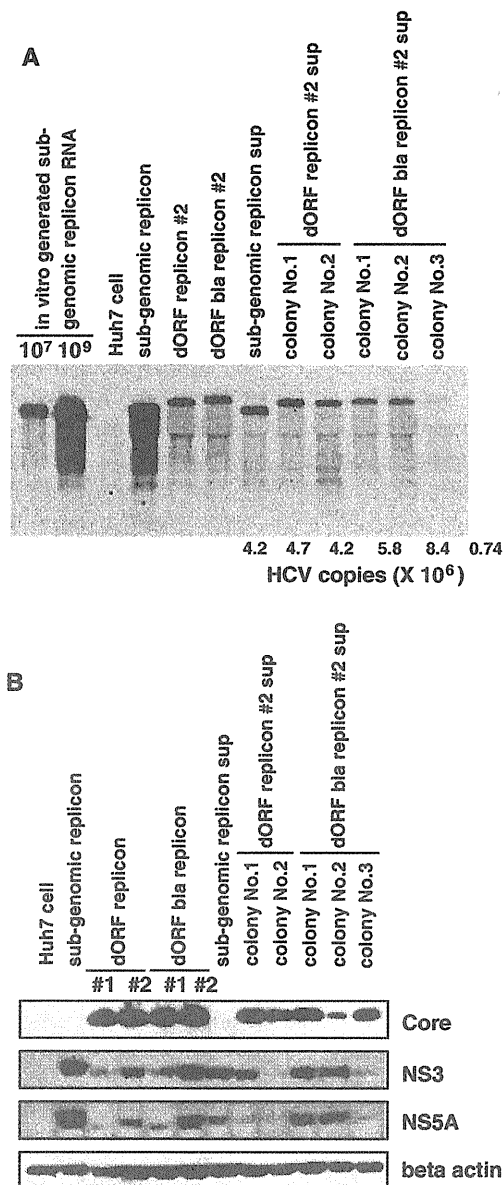

4.2 4.7 4.2 5.8 8.4 0.74
HCV copies (X 10^6)

B

Core

NS3

NS5A

beta actin

Fig. 5 Northern blot analysis of colonies formed after infection. 10^7, 10^9: amounts of in vitro-generated subgenomic replicon RNA loaded. Numbers below the lanes are the HCV copy number per μg of total RNA (A). Huh-7 cells, subgenomic replicon cells, dORF replicon cell #2, dORF bla replicon cell #2, subgenomic replicon sup: colony from cells transduced with subgenomic replicon supernatant, colony No.1, 2 of dORF replicon #2 sup: colonies from cells infected with dORF replicon #2 supernatant, colony No.1, 2, and 3 of dORF bla replicon #2 sup: colonies from cells infected with dORF bla replicon #2 supernatant. Western blot analysis of colonies formed after infection (B). The order of the lanes is identical to that for the northern blot, except for the dORF and dORF bla replicons, which represent two clones in this figure

clones of the same dORF replicon cells, which may have been due to the accumulation of different mutations in the structural region, although we have not yet confirmed this
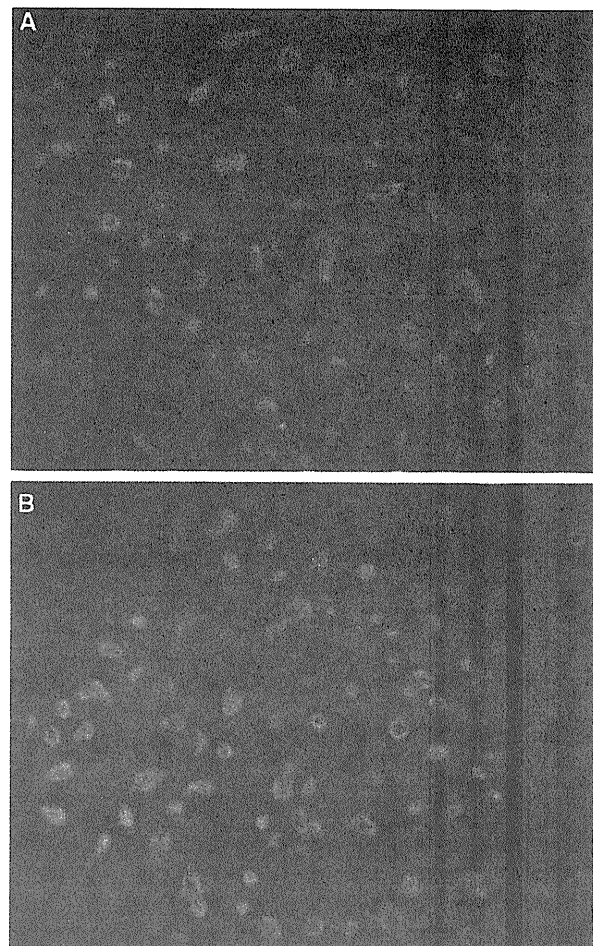

Fig. 6 Detection of beta-lactamase activity in dORF replicon cells. Parental dORF bla replicon #2 cell (A) and colony no. 3 cloned from cells infected with dORF bla replicon #2 cell supernatant (B). Blue fluorescence shows high beta-lactamase activity, indicating that the reporter gene functioned normally after infection

hypothesis. We also observed colonies being formed by cells that were treated with supernatant containing subgenomic replicons, and these colonies most likely represent the so-called "non-specific transduction" of the subgenomic replicon. Although this dORF supernatant infection could be blocked by the anti-CD81 antibody reported previously [30], we cannot exclude the possibility that the infection we observed was due to highly efficient "non-specific transduction," as we could not determine whether "non-specific transduction" also could be affected by the anti-CD81 antibody because of the low colony-forming ability of the supernatant of subgenomic replicons.

We also demonstrated that the reporter gene that was inserted in addition to the neomycin resistance gene could be transmitted to the new generation of viruses. This finding raises the possibility of producing sufficient amounts of reporter virus constitutively.

In summary, we established an infectious-particle-producing HCV replicon system. This achievement should yield more precise information about the encapsidation signal of HCV, which was kept intact despite the partitioning of the genome. This system also allows analysis of the pathway of HCV infection, including adsorption of virions to cell-surface receptors, penetration, uncoating, virus particle assembly, and HCV release. Moreover, the dORF replicon system may be used as a convenient tool to investigate the utility of the newly established siRNA system [14, 27] and evaluation of compounds that are effective against subgenomic replicons.

Although we believe that the reason for our success is our new construct, further examination is necessary to verify our findings.

Materials and methods

Construction and RNA transcription

To construct dORF replicon RNA, the second half of the NS2 region of the HCV-R6 strain [25] was replaced in frame with the foot and mouth disease virus (FMDV) 2A protease gene, the neomycin resistance gene, and the encephalomyocarditis virus (EMCV) internal ribosomal entry site (IRES). In addition, the region from NS3 to the beginning of NS5B was replaced with the 1bneo/delS replicon sequence from the N strain of genotype 1b [6](kindly provided by Dr. Seeger). This construct was designated as the "divided open reading frame carrying full genome" (dORF) replicon. The subgenomic replicon construct was also prepared from the R6 strain and also contained the 1bneo/delS replacement. For the reporter assay, the FMDV 2A protease gene and beta-lactamase gene (bla; Invitrogen) were inserted after the remaining NS2 gene to produce the dORF bla replicon construct. Replication-deficient versions of these three replicons were also prepared by deleting 27 nucleotides, including the GDD motif of NS5B polymerase.

In vitro transcription of these replicon RNAs was performed using the MEGAscript kit (Ambion).

Cell culture and electroporation

Huh-7 cells were cultured in DMEM (SIGMA) with 10% fetal bovine serum. Replicon cells were maintained in the same medium supplemented with 300 μg/mL G418 (Invitrogen). These cells were passaged 3 times a week at a 4:1 splitting ratio. Electroporation of replicon RNA was performed as described previously [17]. The subgenomic replicon (1bneo/delS replicon) cells were treated with 1000 IU of IFN-α for 2 months and cloned by the limited

dilution method. Two of these clones were designated as HCV replicon-cured Huh-7 cells F2 and K4. The cell line containing the full-genome replicon of genotype1b, namely the NNC#2 clone [15], was a kind gift from Dr. Shimotohno of Keio University.

Northern blot analysis and quantification of HCV RNA

Total RNA was purified from cells using ISOGEN (Nippon Gene) for northern blot analysis or ABI prizm6100 (Applied Biosystems) for real-time RT-PCR. Purified RNAs were quantified by absorbance at 260 nm. For northern blot analysis, 30 μg of each total RNA was used with a Northern Max Kit (Ambion) according to the manufacturer's instructions. The probe for detection of HCV RNA was a PCR fragment of the NS5B region (nucleotide numbers 7629–7963) that had been biotin-labeled using a BrightStar Psoralen-Biotin Kit (Ambion) according to the manufacturer's instructions. Following hybridization of the membranes, the probe was detected using a BrightStar BioDetect Kit (Ambion) according to the manufacturer's instructions, and luminescence was detected using the LAS1000 detection system (Fujifilm). Measurement of the HCV RNA copy number by real-time RT-PCR was performed using an ABI PRISM 7900 system (Applied Biosystems) as described previously [24].

Western blot analysis

Western blot analysis was carried out using the conventional semi-dry blot method. Cells were lysed with buffer containing 100 mM Tris-HCl (pH 7.4) and 4% sodium dodecyl sulfate. A 10-μg amount of protein from each sample was separated by SDS-PAGE through a 4–20% gradient gel (Invitrogen) and transferred to the membrane according to the gel manufacturer's protocol. The antibodies used in this study were anti-core mouse monoclonal antibody (MAb), anti-E1 MAb, anti-E2 MAb (reported previously; [25]), anti-NS3 antiserum (reported previously; [25]), anti-NS5B antiserum (Upstate), and anti-beta-actin MAb (Abcam). Horseradish peroxidase-labeled anti-mouse and anti-rabbit IgG goat antibodies (Santa Cruz Biotechnology and DAKO, respectively) were used as the secondary antibody. The membranes were treated using an ECL Plus kit (Amersham) according to the manufacturer's instructions, and luminescence was detected using an LAS1000 system (Fujifilm).

Density gradient analysis and core ELISA

Culture supernatants from replicon cells were loaded onto 10–60% sucrose density gradient tubes with or without 10-fold concentration in an Amicon-100 (Millipore). The

tubes were then ultracentrifuged at 100,000 g for 16 h and fractionated. NP-40 was added to the culture supernatants to a final concentration of 0.5%, and they were then incubated at 4°C for 30 min. For electron microscopy, the culture supernatant was concentrated, loaded onto a 60% sucrose cushion, and ultracentrifuged at 100,000 g for 4 h. The interface between the concentrated medium and the sucrose cushion was collected and separated by the density gradient method described above. A 2-mL fraction from 5 ml to 7 mL from the bottom, with a density of 1.1–1.2 g/mL, was examined by electron microscopy after further concentration by the sucrose cushion ultracentrifugation method described above. The amount of core protein in the fractions was quantified using an Ohso ELISA kit in accordance with the manufacturer's instructions.

Electron microscopy

The concentrated fraction of core protein was observed by scanning and transmission electron microscopy. For scanning electron microscopy, the sample was allowed to settle on the surface of a poly-L-lysine-coated glass cover slip for 30 min, and the attached sample was then fixed with 0.1% glutaraldehyde in 0.1 M phosphate buffer (pH 7.4) for 10 min, washed three times with 0.1 M phosphate buffer, and post-fixed with 1% osmium tetroxide in the same buffer for 10 min. After dehydration through a graded series of ethanol, the samples were dried in a freeze dryer (Hitachi ES-2020, Hitachi) using t-butyl alcohol, coated with osmium tetroxide, approximately 2 nm thick, using an osmium plasma coater (NL-OPC80; Nippon Laser and Electronics Laboratory), and then examined using a Hitachi S-4800 field emission scanning electron microscope at an accelerating voltage of 10 kV [23]. For transmission electron microscopy, the sample was allowed to settle on a formvar-coated nickel grid for 10 min, dried in air, incubated with rabbit anti-E2RR6 antibody (prepared as described in the supplementary information), washed with PBS, and then incubated with goat anti-rabbit IgG coupled to 10-nm colloidal gold (British BioCell). After negative staining with 2% uranyl acetate, the sample was examined using a JEM 1200EX transmission electron microscope (JEOL) at an accelerating voltage of 80 kV.

Rabbit anti-E2 RR6 antibody to the HCV-E2 protein was prepared as follows: The E2 gene of HCV type 1b [25] was cloned under the control of the ATI-P7.5 hybrid promoter of vaccinia virus vector pSFB4 and allowed to recombine with the Lister strain of the vaccinia virus to give vector RVV. Rabbits were infected intradermally with 10^8 p.f.u. of RVV, and 2 months later, they received two booster injections with the purified E2 protein. HCV-E2 protein was expressed from the RVV vector and purified by lentil lectin column chromatography and

affinity chromatography using an anti-E2 monoclonal antibody [25].

Infection

A 2.5-ml aliquot of cleared culture supernatants from replicon cells was added to approximately 70% confluent of Huh-7 cells in 25-cm^2 flasks, and the same amount of complete DMEM was added 2 h later. Infected cells were transferred to 75-cm^2 flasks the next day and to four 10-cm dishes 2 days later. G418 at a concentration of 300 μg/mL was added to the medium immediately after the second passage. The three types of Huh-7 cells used in this study included the one purchased from J.C.R.B. and the 2 IFN-cured replicon cell lines F2 and K4 described above. The medium was changed every other day. For the blocking experiment, cells were treated with the anti-CD81antibody as described previously [30]. Cells were fixed with 10% formalin/PBS(-) for 10 min after washing with PBS(-) and staining with 1% crystal violet/PBS(-) for 1 h before washing with water.

Beta-lactamase detection assay

Beta-lactamase activity was detected using a GeneBLAzer In Vivo Detection Kit (Invitrogen) according to the manufacturer's instructions and observed using a fluorescence microscope (Nikon) with UV light excitation.

References

1. Blight KJ, McKeating JA and Rice CM (2002) Highly permissive cell lines for subgenomic and genomic hepatitis C virus RNA replication. J Virol 76:13001-13014
2. Choo QL, Kuo G, Weiner AJ, Overby LR, Bradley DW and Houghton M (1989) Isolation of a cDNA clone derived from a blood-borne non-A, non-B viral hepatitis genome. Science 244:359-362
3. Date T, Kato T, Miyamoto M, Zhao Z, Yasui K, Mizokami M and Wakita T (2004) Genotype 2a hepatitis C virus subgenomic

replicon can replicate in HepG2 and IMY-N9 cells. J Biol Chem 279:22371-6

4. Date T, Miyamoto M, Kato T, Morikawa K, Murayama A, Akazawa D, Tanabe J, Sone S, Mizokami M and Wakita T (2007) An infectious and selectable full-genome replicon system with hepatitis C virus JFH-1 strain. Hepatol Res 37:433-443

5. Frolova E, Frolov I and Schlesinger S (1997) Packaging signals in alphaviruses. J Virol 71:248-258

6. Guo J, Bichko VV and Seeger C (2001) Effect of alpha interferon on the hepatitis C virus replicon. J Virol 75:8516-8523

7. Ikeda M, Yi M, Li K and Lemon SM (2002) Selectable subgenomic and genome-length dicistronic RNAs derived from an infectious molecular clone of the HCV-N strain of hepatitis C virus replicate efficiently in cultured Huh7 cells. J Virol 76:2997-3006

8. Jia X-Y, Van Eden M, Busch MG, Ehrenfeld E and Summers DF (1998) Trans-encapsidation of a poliovirus replicon by different picornavirus capsid proteins. J Virol 72:7972-7977

9. Johansen LK and Morrow CD (2000) The RNA encompassing the internal ribosome entry site in the poliovirus 5' nontranslated region enhances the encapsidation of genomic RNA. Virology 273:391-399

10. Kanda T, Basu A, Steele R, Wakita T, Ryerse JS, Ray R and Ray RB (2006) Generation of infectious hepatitis C virus in immortalized human hepatocytes. J Virol 80:4633-4639

11. Kanto T, Hayashi N, Takehara T, Hagiwara H, Mita E, Naito M, Kasahara, A, Fusamoto H and Kamada T (1994) Buoyant density of hepatitis C virus recovered from infected hosts: two different features in sucrose equilibrium density-gradient centrifugation related to degree of liver inflammation. Hepatology 19:296-302

12. Kato T, Furusaka A, Miyamoto M, Date T, Yasui K, Hiramoto J, Nagayama K, Tanaka T and Wakita T (2001) Sequence analysis of hepatitis C virus isolated from a fulminant hepatitis patient. J Med Virol 64:334-339

13. Kato T, Date T, Miyamoto M, Furusaka A, Tokushige K, Mizokami M and Wakita, T (2003) Efficient replication of the genotype 2a hepatitis C virus subgenomic replicon. Gastroenterology 125:1808-1817.

14. Kim M, Shin D, Kim SI and Park M (2006) Inhibition of hepatitis C virus gene expression by small interfering RNAs using a tricistronic full-length viral replicon and a transient mouse model. Virus Res 122:1-10

15. Kishine H, Sugiyama K, Hijikata M, Kato N, Takahashi H, Noshi T, Nio Y, Hosaka M, Miyanari Y, Shimotohno K (2002) Subgenomic replicon derived from a cell line infected with the hepatitis C virus. Biochem Biophys Res Commun 293:993-9

16. Lindenbach BD, Evans MJ, Syder AJ, Wolk B, Tellinghuisen TL, Liu C C, Maruyama T, Hynes RO, Burton DR, McKeating JA and Rice CM (2005) Complete replication of hepatitis C virus in cell culture. Science 309:623-626

17. Lohmann V, Korner F, Koch J, Herian U, Theilmann L and Bartenschlager R (1999) Replication of subgenomic hepatitis C virus RNAs in a hepatoma cell line. Science 285:110-113

18. Lu, HH, Alexander L and Winner E (1995) Construction and genetic analysis if dicistronic Polioviruses containing open reading frames for epitopes of Human Immunodeficiency Virus type 1 gp120. J Virol 69:4797-4806

19. Mattion NM, Reilly PA, DiMichele SJ, Crowley JC and Weeks-Levy C (1994) Attenuated poliovirus strain as a live vector: expression of regions of rotavirus outer capsid protein VP7 by using recombinant Sabin 3 viruses. J Virol 68:3925-3933

20. Pietschmann T, Lohmann V, Kaul A, Krieger N, Rinck G, Rutter G, Strand D and Bartenschlager R (2002) Persistent and transient replication of full-length hepatitis C virus genomes in cell culture. J Virol 76:4008-4021

21. Pietschmann T, Kaul A, Koutsoudakis G, Shavinskaya A, Kallis S, Steinmann E, Abid K, Negro F, Dreux M, Cosset FL and Bartenschlager R (2006) Construction and characterization of infectious intragenotypic and intergenotypic hepatitis C virus chimeras. Proc Natl Acad Sci USA 103:7408-7413

22. Pileri P, Uematsu Y, Campagnoli S, Galli G, Falugi F, Petracca R, Weiner AJ, Houghton M, Rosa D, Grandi G and Abrignani S (1998) Binding of hepatitis C virus to CD81. Science 282:938-941

23. Suzuki H, Murasaki K, Kodama K and Takayama H (2003) Intracellular localization of glycoprotein VI in human platelets and its surface expression upon activation. Bri J Haematol 121:904-912

24. Takeuchi T, Katsume A, Tanaka T, Abe A, Inoue K, Tsukiyama-Kohara K, Kawaguchi R, Tanaka S and Kohara M (1999) Real-time detection system for quantification of hepatitis C virus genome. Gastroenterology 116:636-42

25. Tsukiyama-Kohara K, Tone S, Maruyama I, Inoue K, Katsume A, Nuriya H, Ohmori H, Ohkawa J, Taira K, Hoshikawa Y, Shibasaki F, Reth M, Minatogawa Y and Kohara M (2004) Activation of the CKI-CDK-Rb-E2F pathway in full genome hepatitis C virus-expressing cells. J Biol Chem 279:14531-14541

26. Wakita T, Pietschmann T, Kato T, Date T, Miyamoto M, Zhao Z, Murthy K, Habermann A, Krausslich HG, Mizokami M, Bartenschlager R and Liang TJ (2005) Production of infectious hepatitis C virus in tissue culture from a cloned viral genome. Nat Med 11:791-796

27. Watanabe T, Sudoh M, Miyagishi M, Akashi H, Arai M, Inoue K, Taira K, Yoshiba M and Kohara M (2006) Intracellular-diced dsRNA has enhanced efficacy for silencing HCV RNA and overcomes variation in the viral genotype. Gene Ther 13:883-92

28. Yi MK and Lemon SM (2004) Adaptive mutations producing efficient replication of genotype 1a Hepatitis C virus RNA in normal Huh7 cells. J Virol 78:7904-7915

29. Yi MK, Villanueva RA, Thomas D, Wakita T and Lemon SM (2006) Production of infectious genotype 1a hepatitis C virus (Hutchinson strain) in cultured human hepatoma cells. Proc Natl Acad Sci USA 103:2310-2315

30. Zhong J, Gastaminza P, Cheng G, Kapadia S, Kato T, Burton DR, Wieland SF, Uprichard SL, Wakita T and Chisari FV (2005) Robust hepatitis C virus infection in vitro. Proc Natl Acad Sci USA 102:9294-9299